JOICY APARECIDA ALVES CHAVES

PHYSIOLOGICAL AND BIOCHEMICAL RESPONSES OF TOMATO PLANTS TO WHITE MOLD AFFECTED BY MANGANESE PHOSPHITE

Dissertation presented to the Universidade Federal de Viçosa, as part of the requirements of the Graduate Program in Plant Pathology, to obtain the title of *Magister Scientiae*.

Advisor: Fabrício de Ávila Rodrigues

VIÇOSA – MINAS GERAIS
2020

Ficha catalográfica preparada pela Biblioteca Central da Universidade Federal de Viçosa - Câmpus Viçosa

T
C512p
2020

Chaves, Joicy Aparecida Alves, 1994-
Physiological and biochemical responses of tomato plants to white mold affected by manganese phosphite / Joicy Aparecida Alves Chaves. – Viçosa, MG, 2020.
56f. : il. (algumas color.) ; 29 cm.

Orientador: Fabrício de Ávila Rodrigues.
Dissertação (mestrado) - Universidade Federal de Viçosa.
Referências bibliográficas: f.31-40.

1. Tomate - Resistência a doenças e pragas. 2. Fotossíntese. 3. Mofos brancos. I. Universidade Federal de Viçosa. Departamento de Fitopatologia. Programa de Pós-Graduação em Fitopatologia. II. Título.

CDD 22 ed. 635.64294

JOICY APARECIDA ALVES CHAVES

PHYSIOLOGICAL AND BIOCHEMICAL RESPONSES OF TOMATO PLANTS TO WHITE MOLD AFFECTED BY MANGANESE PHOSPHITE

Dissertation presented to the Universidade Federal de Viçosa, as part of the requirements of the Graduate Program in Plant Pathology, to obtain the title of *Magister Scientiae*.

APPROVED: February 20th, 2020

Joicy Aparecida Alves Chaves
Joicy Aparecida Alves Chaves
Author

Fabrício Ávila Rodrigues
Fabrício de Ávila Rodrigues
Advisor

ACKNOWLEDGMENTS

First of all, I thank God for the blessings and opportunities.

Thanks are due to the Universidade Federal de Viçosa (UFV), Department of Plant Pathology, the Laboratory of Host-Pathogen Interaction, and the Postgraduate Program in Plant Pathology for providing conditions for the development of this research.

I thank Conselho Nacional de Desenvolvimento Científico e Tecnológico (CNPq) and Coordenação de Aperfeiçoamento de Pessoal de Nível Superior (CAPES) for their financial support. This study was financed in part by the Coordenação de Aperfeiçoamento de Pessoal de Nível Superior – Brasil (CAPES) – Finance Code 001.

I want to express my sincere thanks to:

Professor Fabrício de Ávila Rodrigues, a great teacher, and passionate researcher, for their guidance, support, competence, and for all the opportunities enabled.

My colleagues at the Laboratory of Host-Pathogen Interaction for their friendship, knowledge sharing, and contribution to this work.

My friends, Adryelle, Victória, Alessandro, Fábio, and Verônica, for their companionship and help these past two years.

My mom Denís for their constant support, encouragement, and complicity, and love.

All my family and friends that support me during this journey.

UFV employees, especially Mário, Daniel, Delfim, and Bruno.

I thank all who contributed directly or indirectly to this work.

THANK YOU!

BIOGRAPHY

JOICY APARECIDA ALVES CHAVES, daughter of Denís Alves Pereira and Hélio Malaquias Chaves, was born on August 5, 1994, in Ponte Nova, Minas Gerais.

In January 2018, she graduated from Universidade Federal de Viçosa (UFV) with a Bachelor in Agronomy. In March 2018, she started the Master's degree in the Graduate Program in Plant Pathology of the UFV under the guidance of Professor Fabrício de Ávila Rodrigues defending her dissertation on February 20, 2020.

ABSTRACT

CHAVES, Joicy Aparecida Alves, M.Sc., Universidade Federal de Viçosa, February, 2020. **Physiological and biochemical responses of tomato plants to white mold affected by manganese phosphite**. Advisor: Fabrício de Ávila Rodrigues.

Considering the potential of white mold, caused by the fungus *Sclerotinia sclerotiorum* (Lib.) de Bary, to reduce tomato production, this study aimed to determinate the effect of manganese (Mn) phosphite on tomato resistance by assessing the photosynthetic performance (gas exchange and chlorophyll *a* fluorescence), the activities of defense enzymes and those related to the antioxidant metabolism as well as the concentrations of photosynthetic pigments, malondialdehyde (MDA), superoxide anion (O_2^-), and hydrogen peroxide (H_2O_2) on plants challenge with *S. sclerotiorum*. The *in vitro* assays showed that *S. sclerotiorum* mycelial growth was inhibited by Mn phosphite in a dose-response manner. The spray of Mn phosphite reduced white mold severity on the leaves of tomato plants. Additionally, higher foliar Mn concentration was observed on plants sprayed with Mn phosphite. The negative effects of *S. sclerotiorum* infection in the photosynthetic process were mitigated by Mn phosphite application as noticed by the values of net carbon assimilation rate, stomatal conductance to water vapor, transpiration rate, maximal photosystem II quantum yield, and concentration of photosynthetic pigments. The concentrations of MDA, H_2O_2, and O_2^- on infected leaves were lower upon Mn phosphite spray. In general, the activities of defense enzymes and those related to the antioxidant metabolism were higher for the water-sprayed plants infected by *S. sclerotiorum* in comparison to those sprayed with Mn phosphite. Based on the results of this study, the application of Mn phosphite may represent a feasible alternative for white mold management in tomato plants.

Keywords: *Sclerotinia sclerotiorum*. Alternative control. Photosynthesis. Host resistance

RESUMO

CHAVES, Joicy Aparecida Alves, M.Sc., Universidade Federal de Viçosa, fevereiro de 2020. **Respostas fisiológicas e bioquímicas de plantas de tomate ao mofo branco afetado por fosfito de manganês.** Orientador: Fabrício de Ávila Rodrigues.

Considerando o potencial do mofo branco, causado pelo fungo *Sclerotinia sclerotiorum* (Lib.) de Bary, em reduzir a produção do tomateiro, este trabalho objetivou determinar o efeito do fosfito de manganês (Mn) na resistência do tomateiro através da análise da performance fotossintética (trocas gasosas e fluorescência da clorofila *a*), as atividades das enzimas de defesa e do metabolismo antioxidativo assim como as concentrações de pigmentos fotossintéticos, de aldeído malônico (MDA), superóxido (O_2^-) e peróxido de hidrogénio (H_2O_2) em plantas desafiadas por *S. sclerotiorum*. *In vitro*, o fosfito de Mn inibiu o crescimento micelial de *S. sclerotiorum*. A aplicação de fosfito de Mn reduziu a severidade do mofo branco em folhas de tomate. Além disso, maior concentração foliar de Mn foi observada em plantas pulverizadas com esse produto. Os efeitos negativos da infecção por *S. sclerotiorum* no processo fotossintético das plantas foram mitigados com a aplicação de fosfito de Mn, demonstrados pelos valores da taxa líquida de assimilação de CO_2, condutância estomática, taxa de transpiração, da máxima eficiência quântica do fotossistema II, e concentração de pigmentos fotossintéticos. As concentrações de MDA, H_2O_2 e O_2^- nas plantas infectadas foi menor com a pulverização do fosfito de Mn. De modo geral, a atividade das enzimas de defesa e do metabolismo antioxidativo foram maiores para as plantas pulverizadas com água e infectadas por *S. sclerotiorum* em relação às pulverizadas com fosfito de Mn. Baseado nos resultados encontrados neste estudo, a aplicação de fosfito de Mn pode se apresentar como uma alternativa viável no manejo do mofo branco em tomateiro.

Palavras-chave: *Sclerotinia sclerotiorum*. Controle alternativo. Fotossíntese. Resistência da planta

SUMMARY

INTRODUCTION

Tomato (*Solanum lycopersicum* L.) production can be negatively affected by the occurrence of white mold, caused by the fungus *Sclerotinia sclerotiorum* (Lib.) de Bary (Boland and Hall, 1994; Lobo Junior et al., 2000; Aguiar et al., 2014). Aside from tomato, more than 400 plant species, including cultivated and wild species, are infected by *S. sclerotiorum* (Boland and Hall, 1994). On leaves, the white mold symptoms start as water-soaked lesions that rapidly expand and turn into necrotic lesions over which intense white cottony fungal mycelium can be noticed (Bolton et al., 2006; Heffer Link and Johnson, 2007). White mold control is challenging to achieve due to the large host range of *S. sclerotiorum* and its great capacity to survive under different environmental conditions and production systems (Bolton et al., 2006; Ferreira et al., 2019). Furthermore, *S. sclerotiorum* produces sclerotia, which are melanized survival structures composed of compact mycelium, which can persist viable in the soil and crop debris for many years (Bolton et al., 2006; Heffer Link and Johnson, 2007).

Integrated management of white mold involves cultural, chemical, and biological methods (Bardin and Huang, 2001; Willbur et al., 2019). Tomato hybrids with resistance to white mold are not available to growers, and white mold control relies on fungicides application (Bolton et al., 2006; Aguiar et al., 2014). Continued application of fungicides has several negative consequences including human and animal health risks, environment contaminations (Damalas and Eleftherohorinos, 2011), and the development of fungicide-resistant isolates of *S. sclerotiorum* (Lehner et al., 2015; Firoz et al., 2016; Liu et al., 2018). In this context, induced host resistance emerges as an interesting strategy for disease control. This approach consists of enhancing the plant defense mechanisms against pathogens attack by abiotic or biotic agents (Vallad and Goodman, 2004; Walters et al., 2013; Alexandersson et al., 2016).

Phosphite ($H_2PO_3^-$), an inorganic salt of the phosphorous acid (H_3PO_3) that can systematically move in the plant tissues, has been used as fertilizer and fungicide in many

commercial crops (Goméz-Merino and Trejo-Téllez, 2015; Achary et al., 2017). Diseases caused by oomycetes, bacteria, and fungus had their intensities reduced by phosphites application (Araújo et al., 2010, 2015; Lobato et al., 2010; Eshraghi et al., 2011; Dalio et al., 2014; Percival and Banks, 2015; Monteiro et al., 2016; Cerqueira et al., 2017; Fagundes-Nacarath et al., 2018ab). The phosphite's mode of action includes its direct inhibition of pathogen growth or the potentiation of host defense mechanisms (*e.g.*, increase on the activities of defense-related enzymes, production of phytoalexins, phenolic compounds, lignin, and reactive oxygen species (ROS)) (Daniel and Guest, 2006; Lobato et al., 2010; Eshraghi et al., 2011; Dalio et al., 2014; Liu et al., 2016). The spray of manganese (Mn) phosphite onto coffee seedlings reduced rust severity as a result of an increase in polyphenoloxidase activity (Monteiro et al., 2016). Phosphite application on common bean plants resulted in an increase in the activities of superoxide dismutase, chitinase, β-1,3-glucanase, and peroxidase as well as high concentrations of total soluble phenolics and lignin (Costa et al., 2017). In addition, phosphite inhibited the mycelial growth of *Colletotrichum lindemuthianum* in vitro (Costa et al., 2017). According to Lobato et al. (2010), the inhibition of pathogen growth by phosphites are linked to several factors such as the concentration of phosphite anion, nature of the phosphite cation, acidification of the medium, and the pathogen's lifestyle.

In addition to the biochemical effects related to phosphites application, they can potentially attenuate the physiological dysfunction occurring on plants infected by pathogens (Dalio et al., 2014; Percival and Banks, 2015; Cerqueira et al., 2017; Fagundes-Nacarath et al., 2018a, Novaes et al., 2019). Phosphite-treated horse chestnut plants displayed lower lesion size caused by bleeding canker and higher chlorophylls concentration as well as great values of the maximum PSII quantum efficiency parameter (F_v/F_m) (Percival and Banks, 2015).

Phosphite salts containing potassium, manganese (Mn), zinc, copper, and calcium are available in the market and are used as a source of macro and micronutrients for plants rather

than a source of phosphorus (Dalio et al., 2012; Goméz-Merino and Trejo-Téllez, 2015; Achary et al., 2017). The Mn is an essential micronutrient for plant growth considering its role as a co-factor of the phenylalanine ammonia-lyase and superoxide dismutase and also for being involved in both photosynthetic and biochemical apparatus of plants (Millaleo et al., 2010).

Considering the importance of white mold to negatively impact tomato yield and the lack of information in the literature regarding the potential of Mn phosphite to reduce the disease symptoms, the present study aimed to investigate the effect of this phosphite to increase tomato resistance to white mold by assessing the photosynthetic and the biochemical performance of tomato plants challenged or not with *S. sclerotiorum*.

MATERIAL AND METHODS

Plant growth

Tomato seeds from cultivar Santa Cruz Kada (Isla Sementes, São Paulo, Brazil), susceptible to *S. sclerotiorum*, were sown in polystyrene trays containing Tropstrato® substrate (Vida Verde, Mogi Mirim, São Paulo, Brazil) composed of a mixture of pine bark, peat, and expanded vermiculite (1:1:1). Fifteen days after emergence, seedlings were transplanted to plastic pots containing 2 kg of substrate. Plants were kept under greenhouse conditions (temperature of 30 ± 5°C, relative humidity of 65 ± 5%, and 900 ± 15 μmol photons m^{-2} s^{-1} natural photosynthetically active radiation). Plants were fertilized weekly with 100 ml of a nutrient solution composed, in mg per Litter (L), of 192 KCl, 104.52 K_2SO_4, 150.37 $MgSO_4$, 61 CH_4N_2O, 100 NH_4NO_3, 0.27 $(NH_4)_6MO_7O_{24}$, 1.61 H_3BO_3, 6.67 $ZnSO_4$, 1.74 $CuSO_4$, 4.10 $MnCl_2$, 4.08 $FeSO_4$, and 5.58 ethylenediaminetetra acetic acid (EDTA). Plants were watered as needed.

Fungal growth, plant inoculation, and treatments

The isolate DFP-UFV *Ss*12 of *S. sclerotiorum* was used to inoculate the plants. Sclerotia were produced in carrots according to Novaes et al. (2019). For inoculum production, one sclerotia was transferred to each Petri dish containing potato-dextrose-agar (PDA) medium (20 g of dextrose, 20 g agar, and 200 g of fresh potato per L of distilled water) and kept in a growth chamber (20°C and 12h photoperiod) for five days. Plants were sprayed with water (control) and manganese (Mn) phosphite (1 L ha^{-1}, Phytogard® Mn (30% P_2O_5 and 9% Mn), Stoller do Brasil S.A., Cosmópolis, Brazil) (15 ml per plant) at 48 h before being inoculated with *S. sclerotiorum*. Four leaflets of the third and fourth leaves, from bottom to top, of each plant per replication of each treatment were inoculated with a plug (5 mm in diameter) of PDA medium obtained from the edge of a five-day-old colony of *S. sclerotiorum*. Each PDA plug was placed between the primary and secondary veins of each leaflet and gently pressed with the index finger. After inoculation, plants were kept in a plastic mist growth chamber (temperature of 28 ± 2°C (day) and 17 ± 2°C (night) and relative humidity maintained at 92 ± 3% using a misting system with nozzles (model NEB-100, KGF, São Paulo, Brazil) that sprayed mist every 30 min above plants canopies) inside the greenhouse during the experiments.

***In vitro* assays**

The sensitivity of *S. sclerotiorum* to Mn phosphite was evaluated *in vitro* using different concentrations (0, 0.3125, 0.625, 1, 1.25, 2.5, 5, 10, and 20 ml L^{-1} of PDA medium) of this product. The fungicide Fluazinam, known to inhibit the mycelial growth of *S. sclerotiorum*, at the same concentrations used for the Mn phosphite treatment was considered the positive control. The products were added to the PDA medium, which was poured into the Petri dishes (20 mL per plate). The PDA plug (5 mm in diameter), containing fungal mycelia obtained from the edge of a five-day-old *S. sclerotiorum* colony, was placed in the center of each Petri dish,

which was kept in a growth chamber (20°C and 12 hours (h) photoperiod). Fungal colony growth was measured in two orthogonal directions using a digital caliper at 24, 36, 48, and 60 h later. The effective concentration for 50% inhibition of mycelial growth (EC_{50}) was determined. A linear regression of the percent of inhibition versus the logarithm in the base 10 of Mn phosphite concentration was performed (Lehner et al., 2015).

Evaluation of white mold severity

The leaflets of the third leaf of plants from the replications of each treatment were collected at 24, 36, 60, and 84 hours after inoculation (hai), scanned at 600 dpi resolution, and the obtained images were processed using the software QUANT (Vale at al., 2003) to quantify the white mold severity (WMS). The area under disease progress curve (AUDPC) for each leaflet of plants from the replications of each treatment was calculated using the trapezoidal integration of the disease progress curve according to Shaner and Finney (1977).

Determination of foliar Mn concentration

The foliar Mn concentrations were determined according to Mesquita et al. (2019) with few modifications. Leaf samples from plants from the replications of each treatment were collected at 96 hai, dried at 65ºC for 72 h, and ground in a ball mill (TECNAL TE 350, Piracicaba, SP, Brazil) for 1 min. Leaf tissue was digested with a nitric-perchloric acid solution, and foliar Mn concentration was determined by optical emission spectrometry with inductively coupled plasma (ICP-OES) (DV8300, PerkinElmer).

Determination of the leaf gas exchange parameters

The leaf gas exchange parameters were determined in one leaflet of the third leaf of each plant (four leaflets per treatment) per replication of each treatment at 12, 36, and 60 hai.

Measurements were also taken from one non-inoculated leaflet from the third leaf at these same evaluations time. The net carbon assimilation rate (A), stomatal conductance to water vapor (g_s), internal CO_2 concentration (C_i), and transpiration rate (E) were estimated from 09:00 to 12:00 h under artificial and saturating photon irradiance (1,000 μmol m^{-2} s^{-1}) and an external CO_2 concentration of 400 μmol mol^{-1} using a portable open-system infrared gas analyzer (LI-6400, LI-COR Inc., Lincoln, NE, USA). All measurements were performed by setting the block temperature at 25°C.

Chlorophyll (Chl) *a* fluorescence imaging

Images and parameters of Chl *a* fluorescence were obtained from one leaflet of the third leaf of each plant per replication of each treatment at 24, 36, 60, and 84 hai using the Imaging-PAM fluorometer and the Imaging Win software MAXI version (Heinz Walz GmbH, Effeltrich Germany). Plants were adapted to darkness for 1 h and then placed individually in support at a distance of 18.5 cm from the CCD ("charge-coupled device") camera to obtain images at the resolution of 640 × 480 pixels. The leaflets were exposed to a light pulse intensity of 0.5 μmol m^{-2} s^{-1}, 100 μs, 1 Hz to obtain the initial fluorescence (F_0). Next, a saturating white light pulse of 2,400 μmol m^{-2} s^{-1} (10 Hz) was emitted for 0.8 s to determine the maximum fluorescence emission (F_m). Based on these initial measurements, the maximum PS II photochemical efficiency of the dark-adapted leaflets was estimated through the variable-to-maximum Chl *a* fluorescence ratio as following: $F_v/F_m = [(F_m - F_0)/F_m)]$. Next, the leaflets were exposed to actinic photon irradiance (531 μmol m^{-2} s^{-1}) for 120 s to obtain the steady-state fluorescence yield (F_s), after which a saturating white light pulse (2,400 μmol m^{-2} s^{-1}; 0.8 s) was applied to achieve the light-adapted maximum fluorescence (F_m'). The light-adapted initial fluorescence (F_0') was estimated according to Oxborough and Baker (1997). Based on Kramer et al. (2004), the energy that was absorbed by the PS II for the following three yield components for

dissipative processes was calculated as follows: the photochemical yield [Y(II) = (F_m' - F_s)/F_m')], the yield for dissipation by down-regulation [Y(NPQ) = (F_s/F_m') - (F_s/F_m)], and the yield for other non-photochemical (non-regulated) losses [Y(NO) = F_s/F_m]. The apparent electron transport rate was calculated as ETR = Y(II) × PPFD × f × α according to Baker (2008).

Determination of photosynthetic pigments concentration

Five squared pieces of leaflets (1 cm^2) were punched from one leaflet of the third leaf of each plant per replication of each treatment at 24, 36, 60, and 84 hai to determine the concentrations Chl *a*, Chl *b*, and carotenoids. Leaflets samples were immersed in glass tubes containing 5 ml of dimethyl sulfoxide (DMSO) solution (saturated with calcium carbonate ($CaCO_3$), 5 g L^{-1}), and kept in the dark at room temperature for 24 h. The absorbance of the extracts was read at 480, 649, and 665 nm in a spectrophotometer using the $CaCO_3$ saturated solution of DMSO as a blank. The concentrations of Chl *a*, Chl *b*, and carotenoids were calculated according to Wellburn (1994).

Biochemical assays

For all biochemical assays, four leaflets of the third and fourth leaves, from bottom to top, of each plant per replication of each treatment were collected at 12, 24, 48, 72, and 96 hai. Leaf samples were kept in liquid nitrogen during sampling and stored at -80°C until further analysis.

Determination of antioxidant enzymes activities

To determine the activities of ascorbate peroxidase (APX) (EC 1.11.1.11), catalase (CAT) (EC 1.11.1.6), peroxidase (POX) (EC 1.11.1.7), superoxide dismutase (SOD) (EC 1.15.1.1), and glutathione reductase (GR) (EC 1.8.1.7) a total of 0.2 g of homogenized leaflets tissues were ground into a fine powder with liquid nitrogen in a mortar and pestle. The fine powder was

homogenized in 2 ml of a solution containing 50 mM of potassium phosphate buffer (pH 6.8), 0.1 mM ethylenediaminetetra acetic (EDTA), 1 mM phenylmethylsulfonyl fluoride (PMSF), and 2% (w/v) polyvinylpyrrolidone (PVP). The homogenized material was centrifuged at 12,000 *g* for 15 min at 4°C, and the supernatant was used as the crude enzyme extract. The SOD activity was determined by measuring its ability to photochemically reduce nitroblue tetrazolium (NBT) as described by Beauchamp and Fridovich (1971). The reaction was initiated by adding the crude enzyme extract to a mixture containing 50 mM potassium phosphate buffer (pH 7.8), 14 mM methionine, 75 µM NBT, 0.1 mM EDTA, and 2 µM riboflavin. Samples were light-exposed for 7 min, and the production of formazan blue, resulting from the photoreduction of NBT, was measured at 560 nm with a spectrophotometer (Giannopolitis and Ries, 1977). Samples kept in the dark for 7 min served as a blank. One unit of SOD was defined as the amount of enzyme necessary to inhibit NBT photoreduction by 50%. The CAT activity was determined by adding the crude enzyme extract to a reaction mixture containing 50 mM potassium phosphate buffer (pH 7.0) and 20 mM hydrogen peroxide (H_2O_2). The determination of CAT activity was based on the rate of H_2O_2 decomposition measured in the spectrophotometer at 240 nm for 1 min at 25°C (Cakmak and Marschner, 1992). An extinction coefficient of 36 M^{-1} cm^{-1} was used to calculate CAT activity (Anderson et al., 1995). POX activity was assayed by determining the pyrogallol oxidation as proposed by Kar and Mishra (1976). The reaction was started after the addition of the crude enzyme extract to a reaction mixture containing 25 mM potassium phosphate (pH 6.8), 20 mM pyrogallol, and 20 mM H_2O_2. The POX activity was determined by the absorbance of colored purpurogallin recorded for 1 min at 420 nm at 25°C. The extinction coefficient of 2.47 mM^{-1} cm^{-1} (Chance and Maehley, 1955) was used to calculate POX activity. The APX activity assay followed that described by Nakano and Asada (1981). The crude enzyme extract was added to a mixture containing 50 mM phosphate buffer (pH 7.0), 0.5 mM ascorbic acid, and 0.1 mM H_2O_2. The rate of ascorbate

oxidation was measured by recording the absorbance at 290 nm for 1 min. The extinction coefficient of 2.8 mM^{-1} cm^{-1} (Nakano and Asada, 1981) was used to calculate APX activity. In order to determine GR activity, the reaction was started after the addition of the crude enzyme extract to a mixture containing 50 mM potassium phosphate (pH 7.8), 1 mM oxidized glutathione (GSSG), and 0.75 mM NADPH prepared in 0.5 mM Tris-HCl buffer (pH 7.5) according to Carlberg and Mannervik (1985). The decrease in absorbance was determined at 340 nm for 1 min at 30°C. The extinction coefficient of 6.22 mM^{-1} cm^{-1} was used to calculate GR activity (Foyer and Halliwell, 1976). Enzymes activities were expressed in a protein-basis whose concentration was determined according to Bradford (1976).

Determination of defense-related enzymes activities

A total of 0.2 g of homogenized leaflets tissues were ground with liquid nitrogen using a mortar and pestle to obtain the powder to determine the activities of chitinase (CHI) (EC 3.2.1.14), *β*-1,3-glucanase (GLU) (EC 3.2.1.39), phenylalanine ammonia-lyase (PAL) (EC 4.3.1.5), polyphenoloxidase (PPO), and lipoxygenase (LOX) (EC 1.13.11.12). The fine powder was homogenized in 2 ml of a solution containing 50 mM potassium phosphate buffer (pH 6.8), 1 mM EDTA, 1 mM PMSF, and 2% (w/v) PVP. The homogenate was centrifuged at 12,000 *g* for 15 min at 4°C, and the supernatant was collected to be used to determine enzymes activity. CHI activity was determined by adding the crude enzyme extract to a reaction mixture containing 50 mM sodium acetate buffer (pH 5.0) and 0.1 mM *p*-nitrophenyl-β-*D*-*N*-*N'*-diacetylchitobiose (Harman et al., 1993). The reaction mixture was incubated in a water bath at 37°C for 2 h, and the reaction was terminated by the addition of 0.2 M sodium carbonate. For the control samples, the sodium carbonate was added soon after the addition of the crude enzyme extract to the reaction mixture. The absorbance of the product released by CHI was measured at 410 nm. The extinction coefficient of 7×10^3 mM^{-1} cm^{-1} was used to calculate CHI activity. GLU activity

was determined after adding the crude enzyme extract to a reaction mixture containing 50 mM sodium acetate buffer (pH 5.0) and laminarin (1 mg/mL) (Lever, 1972). The reaction mixture was incubated in a water bath for 30 min at 45°C. Afterward, this mixture was added to a reaction mixture of dinitrosalicylic acid (DNS). This reaction mixture was then incubated in a water bath for 10 min at 90°C and then cooled in an ice bath until it reached 25°C. The absorbance was measured at 540 nm. A similar procedure was used for the control samples except that the first incubation was excluded. For PAL activity, the crude enzyme extract reacted with a reaction mixture containing 25 mM Tris-HCl buffer (pH 8.8) and 25 mM *L*-phenylalanine. The reaction mixture was incubated at 40°C for 3 h. For the control samples, the extract was replaced by the Tris-HCl buffer. The reaction was stopped by adding 6 N HCl. The absorbance of *trans*-cinnamic acid derivatives was recorded at 290 nm. The extinction coefficient of 100 M^{-1} cm^{-1} was used to calculate PAL activity (Guo et al., 2007). PPO activity was determined using the same procedure as for POX, but H_2O_2 was omitted from the reaction mixture. LOX activity was determined by adding the crude enzyme extract to a reaction mixture containing 50 mM sodium phosphate buffer (pH 6.5) and 50 µM sodium linoleate. The reaction mixture was incubated at 25°C, and the absorbance of the product released by LOX for 1 min was measured at 234 nm. The extinction coefficient of 25000 M^{-1} cm^{-1} was used to calculate LOX activity (Axelrod et al., 1981). These enzyme activities were expressed on a protein basis, and protein concentration was determined according to Bradford (1976).

Determination of malondialdehyde (MDA) concentration

Oxidative damage in the leaflets tissues was estimated as the concentration of total 2-thiobarbituric acid (TBA) reactive substances and expressed as equivalents of MDA (Cakmak and Horst, 1991). A total of 0.1 g of leaflets tissues was ground into a fine powder using a mortar and pestle with liquid nitrogen and homogenized in 2 ml of 0.1% (w/v) trichloroacetic

acid (TCA) solution in an ice bath. The homogenate was centrifuged at 12,000 *g* for 15 min at 4°C. After centrifugation, a total of 250 µl of the supernatant was reacted with 750 µl of TBA solution (0.5% in 20% TCA) for 60 min in a boiling water bath at 95°C. After this period, the reaction was stopped in an ice bath. The samples were centrifuged at 10,000 *g* for 10 min, and the specific absorbance was determined at 532 nm. The non-specific absorbance was estimated at 600 nm and subtracted from the specific absorbance value. The extinction coefficient of 155 mM^{-1} cm^{-1} (Heath and Packer, 1968) was used to calculate MDA concentration.

Determination of superoxide (O_2^-) concentration

A total of 0.2 g of leaflets tissues was ground into a fine powder in a mortar and pestle with liquid nitrogen, homogenized in 2 ml of a solution containing 100 mM sodium phosphate buffer (pH 7.2), and 1 mM sodium diethyldithiocarbamate (SDD). The homogenate was centrifuged at 22,000 *g* for 20 min at 4°C, and the supernatant was used to determine the O_2^- concentration according to Chaitanya and Naithani (1994).

Determination of hydrogen peroxide (H_2O_2) concentration

A total of 0.1 g of leaflets tissues was ground into a fine powder in liquid nitrogen and homogenized in 2 ml of 0.1% (w/v) of TCA. The homogenate was centrifuged at 12,000 *g* for 15 min at 4°C, and the supernatant was used as the crude extract to determine the H_2O_2 concentration. The supernatant was added to a reaction mixture containing 10 mM potassium buffer (pH 7.0) and 1 M of iodide solution and incubated for 10 min. The oxidation product formed was measure a 390 nm (Velikova et al., 2000). A standard curve for H_2O_2 (Sigma-Aldrich, São Paulo, Brazil) was used to determine the H_2O_2 concentration.

Experimental design and statistical analysis

A 2 × 2 factorial experiment, consisting of plants sprayed with water (control) and Mn phosphite (referred as foliar treatments (FT) thereafter) and plant inoculation (PI) (non-inoculated and inoculated plants), was arranged in a completely randomized design with four replications. Each replication corresponded to a plastic pot containing one plant. The experiment was repeated once. All parameters and variables evaluated were subjected to analysis of variance (ANOVA) and means were compared by *F* test ($P \leq 0.05$). For the white mold severity, chlorophyll a fluorescence parameters, concentration of photosynthetic pigments, ANOVA was considered to be 2 × 2 × 4 factorial experiment consisting of two FT, two PI, and four sampling times (ST). For the Mn foliar concentration, the ANOVA was considered a 2 × 2 × 1 factorial experiment consisting of two T, two PI, and one ST. For the leaf gas exchange parameters, the ANOVA was considered a 2 × 2 × 3 factorial experiment consisting of two T, two PI, and three ST. For the biochemical assays, ANOVA was considered a 2 × 2 × 5 factorial experiment consisting of two FT, two PI, and five ST. Data were analyzed using the Minitab software (version 18; Minitab Corporation).

RESULTS

Analysis of variance

The factors foliar treatments (FT), plant inoculation (PI), sampling times (ST) as well as their double interactions were significant for most of the variables and parameters evaluated. The FT × PI × ST interaction was significant for the parameters F_m, F_v/F_m, Y(II), Y (NPQ), Y(NO), ETR as well as for APX and PAL activities and the concentrations of Chl *a*+*b*, CAR, and MDA (Table 1).

In vitro assays

At 60 h after Petri dishes incubation, fungal mycelial growth was reduced by 13, 18, 37, 62, and 81% on PDA medium amended with 0.3125, 0.625, 1, 1.25, 2.5 mL L^{-1}, respectively, of Mn phosphite in comparison to the control treatment (Fig. 1A-F). At concentrations above 5 mL L^{-1}, Mn phosphite completely inhibits fungal mycelial growth (Fig. 1G). There was no fungal growth on PDA medium amended with the fungicide Fluazinam (Fig. 1F). The EC_{50} value was 1.146 mL L^{-1}(Fig. 1I).

Disease evaluation

White mold symptoms were reduced at 36, 60, and 84 hai on the leaflets of tomato plants sprayed with Mn phosphite in contrast to the control treatment (Fig. 2B-D and F-H). Reductions of 82, 80, and 72% at 36, 60, and 84 hai, respectively, in severity were recorded for Mn phosphite-sprayed plants in comparison to plants from the control treatment (Fig. 3A). The AUDPC was significantly reduced by 77% for Mn phosphite-sprayed plants in contrast to plants from the control treatment (Fig. 3J).

Foliar Mn concentration

Non-inoculated and inoculated plants sprayed with Mn phosphite showed significant increases of 53 and 91%, respectively, for foliar Mn concentration compared with the control treatment (Fig. 4).

Leaf gas exchange parameters

The *A* at 36 and 60 hai (45 and 36%, respectively) as well as g_s and *E* at 60 hai (63 and 80%, respectively) significantly increased for Mn phosphite sprayed-plants in comparison to the control treatment (Fig. 5B, D, F, and H). For inoculated plants, *A* was significantly lower by 48% at 60 hai for Mn phosphite treatment and by 47 and 60%, respectively, at 36 and 60 hai for the control treatment in comparison to non-inoculated ones (Fig. 5A and B). At 60 hai, g_s and *E* were significantly lower by 32 and 40%, respectively, for inoculated plants in comparison to the non-inoculated ones from the control treatment (Fig. 5C-D and G-H). For inoculated plants, C_i was significantly higher by 12, 8, and 14% at 12, 36, and 60 hai, respectively, and by 11% at 60 hai for control and Mn phosphite treatments, respectively, in comparison to the non-inoculated plants (Fig. 5E-F).

Chl *a* fluorescence parameters

There was no alteration on the images and on the quantitative analysis of the Chl *a* fluorescence parameters for non-inoculated plants regardless of the treatments and sampling time (Figs. 6, 7A, C, E, G, I, and K). For inoculated leaflets of plants from the control treatment, changes in the images of Chl *a* fluorescence parameters were detected at 24 hai. A progressive loss of the photosynthetic capacity was evident over time as indicated by the black areas in the images. For inoculated plants sprayed with Mn phosphite, alterations in the images of Chl *a* fluorescence parameters were evident only from 36 hai onwards. However, such alterations

were less pronounced when compared to plants from the control treatment (Fig. 6). For inoculated plants sprayed with Mn phosphite, there were significant increases of 22, 18, and 37% for F_v/F_m, of 88, 37, and 110% for Y(II), and of 97, 33, and 109% for ETR at 36, 60, and 84 hai, respectively, in comparison with those from control treatment (Fig. 7B, D, and J). Conversely, there were significant decreases for Y(NPQ) (25 and 15%), respectively, at 36 and 84 hai and for Y(NO) (32, 22, and 35%) at 36, 60, and 84 hai, respectively, for Mn phosphite treatment in comparison to the control treatment (Fig. 7F and H). For inoculated plants from the control treatment, there were significant decreases of 19, 21, and 33% for F_v/F_m, of 45, 45, and 62% for Y(II), and of 49, 44, and 64% for ETR at 36, 60, and 84 hai, respectively, in comparison to the non-inoculated plants (Fig. 7A-D and I-J). Y(NPQ) significantly increased by 20, 59, 54, 68% and Y(NO) by 11, 51, 42, 83% at 24, 36, 60, and 84 hai, respectively, for inoculated Mn phosphite-sprayed plants in comparison to the non-inoculated counterparts (Fig. 7E-H). Inoculated plants from Mn phosphite treatment showed significant reductions of 7 and 5% for F_v/F_m, of 30 and 25% for Y(II), and of 31 and 28% for ETR at 60 and 84 hai, respectively, in comparison to the non-inoculated counterparts (Fig. 7A-B and I-J). Y(NPQ) significantly increased by 76 and 35% and Y(NO) by 16 and 25%, respectively, at 60 and 84 hai for inoculated plants sprayed with Mn phosphite in comparison to the non-inoculated ones (Fig. 7E-H).

Photosynthetic pigments

The Chl *a*+*b* concentration significantly increased by 10 and 30%, respectively, at 60 and 84 hai and the carotenoids concentration by 19 and 44%, respectively, at 60 and 84 hai for the Mn phosphite treatment in comparison to the control treatment (Fig. 8B and D). For inoculated plants, Chl *a*+*b* concentration was significantly lower by 24% at 84 hai and the carotenoids

concentration by 6 and 24%, respectively, at 60 and 84 hai for control treatment in comparison to their non-inoculated counterparts (Fig. 8B and D).

Antioxidant enzymes

For inoculated plants, there were significant decreases in the activities, respectively, of 39 and 28% for SOD at 48 and 72 hai, of 46% for APX at 72 hai, of 46, 45, and 37% for CAT at 12, 24, and 48 hai, of 63 and 56% for POX at 48 and 96 hai, and of 24, 49, and 28% for GR at 12, 24, and 48 hai for the Mn phosphite treatment in comparison to the control treatment (Fig. 9B, D, F, H, and I). Inoculated water-sprayed plants showed significant increases in the activities of SOD at 12, 48, and 72 hai (58, 48, and 79%, respectively), APX at 24, 48, 72 and 96 hai (87, 61, 112, and 190%, respectively), CAT at 12, 24, and 48 hai (47, 91, and 77%, respectively), POX at 48, 72, and 96 hai (65, 137, and 286%, respectively), and GR at 12, 24, and 48 hai (28, 52, and 42%, respectively) in comparison to their non-inoculated counterparts (Fig 9A-J). For Mn phosphite-sprayed and inoculated plants, there were significant increases for the activities of SOD by 34% at 12 hai, APX by 28 and 122% at 12 and 96 hai, respectively, and POX by 149 and 126%, respectively, at 72 and 96 hai in comparison to their non-inoculated counterparts (Fig. 9B, D, and H).

Defense enzymes

The inoculated Mn phosphite-sprayed plants showed significant decreases for the activities of CHI (36 and 31% at 72 and 96 hai, respectively), GLU (61, 64, 57, and 41% at 12, 24, 48, and 72 hai, respectively), PPO (33 and 32% at 48 and 72 hai, respectively), and LOX (33, 32, and 36% at 12, 24, and 48 hai, respectively) in comparison to the control treatment (Fig. 10B, D, H, and J). PAL activity was significantly higher by 133% at 96 hai, for inoculated plants from Mn phosphite treatments in contrast to the control treatment (Fig. 10F). For water-sprayed and

inoculated plants, there were significant increases for the activities of CHI by 55 and 57% at 72 and 96 hai, respectively, GLU by 302, 193, 98, 537, and 173% at 12, 24, 48, 72, and 96 hai, respectively, PPO by 42 and 55% at 48 and 72 hai, respectively, and LOX by 55, 35, and 68% at 12, 48, and 72 hai, respectively, in comparison to their non-inoculated counterparts (Fig 10A-D and G-J). PAL activity was significantly lower by 35 and 70% at 72 and 96 hai, respectively, for inoculated plants control treatment in contrast to the non-inoculated ones (Fig. 10E-F). For inoculated Mn phosphite-sprayed plants, there were increases of 55% for CHI activity at 96 hai and of 224 and 86% for GLU activity at 72 and 96 hai, respectively, in comparison to the non-inoculated counterparts (Fig. 10A-D).

Concentrations of MDA, O_2^-, and H_2O_2

The inoculated Mn phosphite-sprayed plants showed significant decreases in the concentrations of MDA (26, 21, and 35% at 48, 72, and 96 hai, respectively) and O_2^- (27 and 30% at 48 and 72 hai, respectively) (Fig. 11B, D, and F). Inoculated plants sprayed with water showed significant increases of 53, 38, 82, and 105%, respectively, at 24, 48, 72, and 96 hai for MDA concentration, and of 50, 69 and 52%, respectively at 48, 72 and 96 hai for O_2^- concentration, and decreases of 47% at 96 hai for H_2O_2 in comparison to their non-inoculated counterparts (Fig. 11A-F). For the Mn phosphite-sprayed and inoculated plants, there were significant increases of 59 and 52%, respectively, at 72 and 96 hai for MDA concentration and of 43% at 96 hai for O_2^- concentration in comparison to the non-inoculated ones (Fig. 11A-B).

DISCUSSION

The present study brings novel information from the physiological and biochemical perspectives regarding the potential of Mn phosphite in reducing white mold symptoms on tomato plants. Previous studies demonstrated that zinc (Zn) and copper (Cu) phosphites were

efficient in affecting white mold progress in common bean (Fagundes-Nacarath et al., 2018ab). Additionally, other studies reported the potential of phosphites in protecting commercial crops from being infected by oomycetes (Eshraghi et al., 2011; Dalio et al., 2014; Liu et al., 2016; Mulugeta et al., 2019) and other pathogens such as *Ceratocystis fimbriata*, *Cochliobolus miyabeanus*, *Colletotrichum gloeosporioides*, *Fusarium* spp., *Hemileia vastatrix*, *Rhizoctonia solani*, *Streptomyces scabies*, *Sclerotinia sclerotiorum*, and *Pseudomonas syringae* pv. *aesculin* (Araujo et al., 2010, 2015; Lobato et al., 2010; Percival and Banks, 2015; Monteiro et al., 2016; Nascimento et al., 2016; Cerqueira et al., 2017; Novaes et al., 2019).

Phosphites can directly inhibit pathogen growth as well as to potentiate the mechanisms of host defense against their infection (Dalio et al., 2014; Liu et al., 2016). In the present study, the *in vitro* assays showed that *S. sclerotiorum* mycelial growth was inhibited by Mn phosphite in a dose-response manner, suggesting, therefore, its potential to interfer on fungal physiology. Moreover, fungal mycelial growth was completely inhibited at the same Mn phosphite concentration used to spray the plants. The spray of Mn phosphite resulted in lesions of reduced size on tomato leaflets indicating its negative effect on fungal colonization besides a possible direct effect of this product against *S. scleriotiorum* over the leaf surface. The mechanisms by which phosphites inhibit fungal mycelial growth must be elucidated. It has been proposed that phosphites can inhibit fungal growth through inhibition of detrimental phosphorylation reactions (Niere et al., 1994), alteration of nucleotides pools and pentose phosphate metabolism (Barchietto et al., 1989, 1992), and on adenylate synthase (Griffith et al., 1990).

Foliar Mn concentration increased upon Mn phosphite spray onto tomato plants. In general, it was not observed any changes in the photosynthetic or biochemical processes for non-inoculated and Mn phosphite-sprayed plants. Mesquita et al. (2019) reported that sugarcane plants sprayed with solutions containing 5 g L^{-1} Mn or 10 g L^{-1} prepared with $MnSO_4$ showed

reduced orange rust symptoms associated with high *A* and g_s values and attenuation of the oxidative stress imposed by fungal infection on leaves.

Photosynthesis is the major physiological process affected by pathogens infection as reported for many host-pathogen interactions (Aucique-Perez et al., 2014; Tatagiba et al., 2015; Silveira et al., 2015; Rios et al., 2017, 2018; Dias et al., 2018). In the present study, *S. sclerotiorum* infection dramatically decreased photosynthesis on tomato leaflets. The decrease in *A* on leaflets infected by *S. sclerotiorum* may be coupled with stomatal closure (lower g_s values). It was reported that the oxalic acid, a non-host specific toxin determinant of *S. sclerotiorum* pathogenicity, caused guard cell dysfunction and inhibited stomatal closure on the leaves of fava beans plants upon fungal infection (Guimarães and Stotz, 2004). Decreases in *A* linked to increases in C_i indicated biochemical alterations rather than stomatal limitations. Similar findings were reported for wheat-*Pyricularia oryzae* (Aucique-Perez et al., 2014) and soybean-*Phakopsora pachyrhizi* (Rios et al., 2018) interactions were decreases in *A* during fungal infections were not linked to stomatal limitations.

The damage in the photosynthetic apparatus on the leaflets of tomato plants infected by *S. sclerotiorum* was alleviated by Mn phosphite spray. Similarly, common bean plants sprayed with Zn and Cu phosphites had the functionality of their photosynthetic apparatus, and gas exchange capacity increased upon *S. sclerotiorum* infection (Fagundes-Nacarath et al., 2018a). Phosphite treatment helped to preserve *A*, water uptake, Rubisco activity, and maximum rate of electron transport on common beech plants infected by *Phytophtora plurivora* (Dalio et al., 2014).

Among the Chl *a* fluorescence parameters, F_v/F_m reflects the quantum efficiency of photosystem II (PSII) and is an excellent indicator of plant stress (Maxwell & Johnson, 2000). In the present study, *S. sclerotiorum* infection contributed to progressively decrease F_v/F_m and Y(II) values and increase the Y(NO) values suggesting, therefore, photoinhibition and damage

of PSII especially for tomato plants non-sprayed with Mn phosphite. Great Y(NPQ) values indicated that the excess of excitation energy was dissipated as heat as a physiological mechanism of plant photoprotection. The ETR values were dramatically decreased as the lesions of white mold expanded on the leaflets of tomato plants due to the action of cell wall degrading enzymes and non-host-selective toxins released by *S. sclerotiorum* (Bateman and Beer, 1965). In line with this finding, tobacco plants infected by *S. sclerotiorum* displayed high photodamage to the PSII due to the release of oxalic acid (Yang et al., 2014). According to Silveira et al. (2015), decreases on F_v/F_m and ETR values on the leaflets of tomato plants infected by *Xanthomonas gardineri* were linked to increases on Y(NPQ) values demonstrating that heat dissipation was being used to prevent the photoinhibition and damage to the PSII. In the present study, photochemical dysfunction in the leaflets of tomato plants infected by *S. sclerotiorum* was attenuated upon Mn phosphite spray. The decrease in white mold symptoms for plants sprayed with Mn phosphite strongly contributed to a continuous loss in the efficient use of light energy through carbon fixation reactions. Therefore, both the excitation energy directed to photochemical conversion and the protection regulatory mechanisms remained effective during the infection process of *S. sclerotiorum*. Consistent with the results of the present study, common bean plants sprayed with Zn and Cu phosphites and *S. sclerotiorum*-infected showed higher F_v/F_m, Y(II), and ETR values linked to lower Y(NPQ) and Y(NO) values in comparison to non-sprayed plants indicating, therefore, that the photooxidative damage caused by fungal infection was alleviated by the spray of these two phosphites (Fagundes-Nacarath et al., 2018a).

As the white mold lesions expanded and the photodamage increased in the leaflets of tomato plants, the concentration of photosynthetic pigments (Chl *a*, Chl *b*, and Car) decreased. Reductions in the concentration of photosynthetic pigments may be associated with the action of oxalic acid and cell wall degrading enzymes on the leaflets that lead to tissue maceration and

chloroplasts degeneration (Bateman and Beer, 1965; Tariq and Jefferies, 1985). The concentration of photosynthetic pigments from plants sprayed with Mn phosphite was preserved through the time-course of fungal infection, confirming the positive effect of this phosphite to maintain the functionality of photosynthesis on the leaflets of tomato plants. High MDA concentration, a lipid peroxidation marker, was also obtained on leaflets of tomato plants as the white mold symptoms developed for non-sprayed in contrast to Mn phosphite-sprayed plants. Accordingly, Malenčić et al. (2010) reported that MDA concentration gradually increased in soybean leaflets infected by *S. sclerotiorum*.

The reactive oxygen species (ROS) (*e.g.*, hydrogen peroxide (H_2O_2), singlet oxygen ($^1O_2$), superoxide anion (O_2^-), and hydroxyl radical (OH)) are known to be key signaling molecules on plants in response to pathogens infection (Veluchamy et al., 2012; Camejo et al., 2016). The oxalate produced by *S. sclerotiorum* inhibits oxidative burst, rapid and transient production of ROS, at the beginning of fungal infection to favor its pathogenesis (Cessna et al., 2000; Williams et al., 2011, Kabbage et al., 2013). In the present study, there were increases in O_2^- concentration during the infection process of *S. sclerotiorum* on water-sprayed plants. By contrast, the H_2O_2 concentration decreased for non-sprayed and inoculated plants at advanced stage of fungal infection, which might be due to the extended amount of dead leaf tissue. In general, tomato plants sprayed with Mn phosphite and infected by *S. sclerotiorum* displayed similar O_2^- and H_2O_2 concentrations in comparison to non-inoculated plants indicating the potential of this phosphite to reduce the cellular damage caused by *S. sclerotiorum* infection.

Plants have developed an efficient enzymatic system to remove the excess of ROS produced during pathogens infection (You and Chan, 2015). The antioxidant enzymes are localized in different subcellular compartments such as chloroplasts, mitochondria, and peroxisomes (Das and Roychoudhury, 2014). The SOD acts converting O_2^- into O_2 and H_2O_2 while APX, CAT, and POX are responsible for H_2O_2 detoxification (Sharma et al., 2012; Das

and Roychoudhury, 2014). In the ascorbate-glutathione cycle, the GR uses NADPH as a reductant to catalyze the reduction of GSSG to GSH, which is important to the scavenging of H_2O_2 (Sharma et al., 2012; Das and Roychoudhury, 2014). High SOD, CAT, APX, and GR activities were noticed on tomato leaves in response to *Alternaria alternata* infection (Meena et al., 2016). In the present study, the activities of all antioxidant enzymes increased for non-sprayed Mn phosphite plants infected by *S. sclerotiorum*. The inoculated and Mn phosphite-sprayed plants displayed an increase in the activities of SOD, APX, and POX in comparison to their non-inoculated counterparts. Moreover, the increase in the activities of these antioxidative enzymes was lower in contrast to water-sprayed plants infected with *S. sclerotiorum*. Fagundes-Nacarath et al. (2018b) pointed out that Zn and Cu phosphites mediated white mold resistance of common bean plants through an early increase in SOD, POX, APX, and glutathione-S-transferase (GST) activities.

The hydrolytic enzymes CHI and GLU play a key role in the host defense responses because they catalyze the hydrolyzation of carbohydrates chitin and β-1,3-glucan found in fungal cell wall of pathogens (Sánchez-Vallet et al., 2015). For inoculated and water-sprayed plants, CHI activity was high at advanced stage of fungal infection, while GLU activity was kept higher during the entire fungal infection process. The Mn phosphite sprayed-plants displayed higher CHI and GLU activities at advanced stage of fungal infection in contrast to their non-inoculated counterparts. Similarly, common bean plants infected by *S. sclerotiorum* showed high CHI activity regardless of phosphites application (Fagundes-Nacarath et al., 2018b). In the phenylpropanoid pathway, PAL catalyzes the deamination of the amino acid *L*-phenylalanine to produce *trans*-cinnamic acid while the PPO is involved in the oxidation of several phenolics that lead to the production of quinones (Campbell and Sederoff, 1996; Dixon et al., 2002). The higher PAL activity observed on the inoculated plants sprayed with Mn phosphite in comparison to plants from the control treatment at advanced stage of fungal

infection could be possibly linked to the greater foliar Mn concentration considering that this micronutrient is a co-factor of PAL. Increases in PAL activity on grapevine exposed to Mn stress using $MnSO_4$ and infected by *Uncinula necator* were associated with the excess of Mn (Yao et al., 2012). Both PPO and LOX activities increased for inoculated plants non-sprayed with Mn phosphite. Therefore, the reduction in white mold symptoms on the leaflets of tomato plants can be attributed to the direct action of the Mn phosphite against *S. sclerotiorum* considering its inefficiency to prime tomato plants against fungal infection. Consistent with the findings of the present study, Nascimento et al. (2016) reported that K phosphite spray reduced brown spot severity in rice plants without the potentiating the activities of defense enzymes. By contrast, K phosphite spray reduced anthracnose severity on common bean plants by inhibiting fungal mycelial growth as well as helping to increase the activities of defense enzymes (Costa et al., 2017).

Taken together, the results of the present study demonstrated the potential of Mn phosphite to reduce the symptoms of white mold on tomato plants in a scenario where the damage caused by *Sclerotiorum* infection on photosynthesis was greatly constrained. It was noticed that the less white mold symptoms as a result of Mn phosphite spray could be attributed to its direct effect on inhibiting fungal mycelial growth rather than on the potentiation of tomato defense responses. Based on our findings, the preventative application of Mn phosphite may represent a feasible alternative for white mold management in tomato plants.

REFERENCES

Achary, V.M.M., Ram, B., Manna, M., Datta, D., Bhatt, A., Reddy, M.K., Agrawal, P.K., 2017. Phosphite: a novel P fertilizer for weed management and pathogen control. Plant Biotechnol. J. 15, 1493–1508.

Aguiar, R.A., da Cunha, M.G., Lobo Junior, M., 2014. Management of white mold in processing tomatoes by *Trichoderma* spp. and chemical fungicides applied by drip irrigation. Biol. Control 74, 1–5.

Alexandersson, E., Mulugeta, T., Lankinen, Å., Liljeroth, E., Andreasson, E., 2016. Plant resistance inducers against pathogens in Solanaceae species-from molecular mechanisms to field application. Int. J. Mol. Sci. 17, 1673.

Anderson, M.D., Prasad, T.K., Stewart, C.R., 1995. Changes in isozyme profiles of catalase, peroxidase, and glutathione reductase during acclimation to chilling in mesocotyls of maize seedlings. Plant Physiol. 109, 1247–1257.

Araújo, L., Valdebenito-Sanhueza, R.M., Stadnik, M.J., 2010. Avaliação de formulações de fosfito de potássio sobre *Colletotrichum gloeosporioides in vitro* e no controle pós-infeccional da mancha foliar de Glomerella em macieira. Trop. Plant Pathol. 35, 54–59.

Araujo, L., Bispo, W.M.S., Rios, V.S., Fernandes, S.A., Rodrigues, F.A., 2015. Induction of the phenylpropanoid pathway by acibenzolar-*S*-methyl and potassium phosphite increases mango resistance to *Ceratocystis fimbriata* infection. Plant Dis. 99, 447–459.

Aucique-Perez, C.E., Rodrigues, F.A., Moreira, W.R., DaMatta, F.M., 2014. Leaf gas exchange and chlorophyll *a* fluorescence in wheat plants supplied with silicon and infected with *Pyricularia oryzae*. Phytopathology 104, 143-149.

Axelrod, B., Cheesbrough, T.M., Laasko, S., 1981. Lipoxygenases from soybeans. Methods Enzymol. 71, 441-451.

Baker, N.R., 2008. Chlorophyll fluorescence: a probe of photosynthesis in vivo. Annu. Rev. Plant Biol. 59, 89–113.

Barchietto, T., Saindrenan, P., Bompeix, G., 1989. Characterization of phosphonate uptake in two *Phytophthora* spp. and its inhibition by phosphate. Arch. Microbiol. 151, 54–58.

Barchietto, T., Saindrenan, P., Bompeix, G., 1992. Physiological responses of *Phytophthora citrophthora* to a subinhibitory concentration of phosphonate. Pestic. Biochem. Physiol. 42, 151–166.

Bardin, S.D., Huang, H.C., 2001. Research on biology and control of Sclerotinia diseases in Canada 1. Can. J. Plant Pathol. 23, 88–98.

Bateman, D.F., Beer, S.V., 1965. Simultaneous production and synergistic action of oxalic acid and polygalacturonase during pathogenesis by *Sclerotium rolfsii*. Phytopathology 55, 204–211.

Beauchamp, C., Fridovich, I., 1971. Superoxide dismutase: improved assays and an assay applicable to acrylamide gels. Anal. Biochem. 44, 276-287.

Boland, G.J., Hall, R., 1994. Index of plant hosts of *Sclerotinia sclerotiorum*. Can. J. Plant Pathol. 16, 93–108.

Bolton, M.D., Thomma, B.P.H.J., Nelson, B.D., 2006. *Sclerotinia sclerotiorum* (Lib.) de Bary: Biology and molecular traits of a cosmopolitan pathogen. Mol. Plant Pathol. 7, 1–16.

Bradford, M.N., 1976. A rapid and sensitive method for the quantitation of microgram quantities of protein utilizing the principle of protein-dye binding. Anal. Biochem. 72, 248–254.

Cakmak, I., Horst, W.J., 1991. Effect of aluminium on lipid peroxidation, superoxide dismutase, catalase, and peroxidase activities in root tips of soybean (*Glycine max*). Physiol. Plant. 83, 463-468.

Cakmak, I., Marschner, H., 1992. Magnesium deficiency and high light intensity enhance activities of superoxide dismutase, ascorbate peroxidase, and glutathione reductase in bean leaves. Plant Physiol. 98, 1222–1227.

Camejo, D., Guzmán-Cedeño, A., Moreno, A., 2016. Reactive oxygen species, essential molecules, during plant-pathogen interactions. Plant Physiol. Biochem. 103, 10–23.

Campbell, M.M., Sederoff, R.R., 1996. Variation in lignin content and composition. Plant Physiol. 110, 3–13.

Carlberg, I., Mannervik, B., 1985. Glutathione reductase. Methods Enzymol. 113, 484–490.

Cerqueira, A., Alves, A., Berenguer, H., Correia, B., Gómez-Cadenas, A., Diez, J.J., Monteiro, P., Pinto, G., 2017. Phosphite shifts physiological and hormonal profile of Monterey pine and delays *Fusarium circinatum* progression. Plant Physiol. Biochem. 114, 88–99.

Cessna, S.G., Sears, V.E., Dickman, M.B., Low, P.S., 2000. Oxalic acid, a pathogenicity factor for *Sclerotinia sclerotiorum*, suppresses the oxidative burst of the host plant. Plant Cell 12, 2191–2199.

Chaitanya, K.S.K., Naithani, S.C., 1994. Role of superoxide, lipid peroxidation and superoxide dismutase in membrane perturbation during loss of viability in seeds of *Shorea robusta* Gaertn.f. New Phytol. 126, 623–627.

Chance, B., Maehley, A.C., 1955. Assay of catalases and peroxidases. Methodslever Enzymol. 2, 764–775.

Costa, B.H.G., Resende, M.L.V., Monteiro, A.C.A., Ribeiro Júnior, P.M., Botelho, D.M.S., Silva, B.M., 2017. Potassium phosphites in the protection of common bean plants against anthracnose and biochemical defence responses. J. Phytopathol. 166, 95–102.

Dalio, R.J.D., Ribeiro Junior, P.M., Resende, M.L.V., Silva, A.C., Blumer, S., Pereira, V.F., Osswald, W., Pascholati, S.F., 2012. O triplo modo de ação dos fosfitos em plantas. Rev. An. Patol. Plantas 20, 206-243.

Dalio, R.J.D., Fleischmann, F., Humez, M., Osswald, W., 2014. Phosphite protects *Fagus sylvatica* seedlings towards *Phytophthora plurivora* via local toxicity, priming, and facilitation of pathogen recognition. PLoS One 9, e87860.

Damalas, C.A., Eleftherohorinos, I.G., 2011. Pesticide exposure, safety issues, and risk assessment indicators. Int. J. Environ. Res. Public Health 8, 1402–1419.

Daniel, R., Guest, D., 2006. Defence responses induced by potassium phosphonate in *Phytophthora palmivora*-challenged *Arabidopsis thaliana*. Physiol. Mol. Plant Pathol. 67, 194–201.

Das, K., Roychoudhury, A., 2014. Reactive oxygen species (ROS) and response of antioxidants as ROS-scavengers during environmental stress in plants. Front. Environ. Sci. 2, 53.

Dias, C.S., Araujo, L., Chaves, J.A.A., DaMatta, F.M., Rodrigues, F.A., 2018. Water relation, leaf gas exchange and chlorophyll *a* fluorescence imaging of soybean leaves infected with *Colletotrichum truncatum*. Plant Physiol. Biochem. 127, 119–128.

Dixon, R.A., Achnine, L., Kota, P., Liu, C.J., Reddy, M.S.S., Wang, L., 2002. The phenylpropanoid pathway and plant defence - a genomics perspective. Mol. Plant Pathol. 3, 371–390.

Eshraghi, L., Anderson, J., Aryamanesh, N., Shearer, B., McComb, J., Hardy, G.E.S.J., O'Brien, P.A., 2011. Phosphite primed defence responses and enhanced expression of defence genes in *Arabidopsis thaliana* infected with *Phytophthora cinnamomi*. Plant Pathol. 60, 1086–1095.

Fagundes-Nacarath, I.R.F., Debona, D., Brás, V.V., Silveira, P.R., Rodrigues, F.A., 2018a. Phosphites attenuate *Sclerotinia sclerotiorum*-induced physiological impairments in common bean. Acta Physiol. Plant. 40, 198.

Fagundes-Nacarath, I.R.F., Debona, D., Oliveira, A.T.H., Hawerroth, C., Rodrigues, F.A., 2018b. Biochemical responses of common bean to white mold potentiated by phosphites. Plant Physiol. Biochem. 132, 308–319.

Ferreira, L.U., Ribeiro, V.A., Melo, P.G.S., Lobo Junior, M., Costa, J.G.C., Pereira, H.S., Melo, L.C., Souza, T.L.P.O., 2019. Comparison of inoculation methods for selecting common bean genotypes with physiological resistance to white mold. Trop. Plant Pathol. 44, 65–72.

Firoz, M.J., Xiao, X., Zhu, F.X., Fu, Y.P., Jiang, D.H., Schnabel, G., Luo, C.X., 2016. Exploring mechanisms of resistance to dimethachlone in *Sclerotinia sclerotiorum*. Pest Manag. Sci. 72, 770–779.

Foyer, C.H., Halliwell, B., 1976. The presence of glutathione and glutathione reductase in chloroplasts: a proposed role in ascorbic acid metabolism. Planta 133, 21-25.

Giannopolitis, C.N., Ries, S.K., 1977. Superoxide dismutases I. Occurrence in higher plants. Plant Physiol. 59, 309-314.

Gómez-Merino, F.C., Trejo-Téllez, L.I., 2015. Biostimulant activity of phosphite in horticulture. Sci. Hortic. 196, 82–90.

Griffith, J.M., Smillie, R.H., Grant, B.R., 1990. Alterations in nucleotide and pyrophosphate levels in *Phytophthora palmivora* following exposure to the antifungal agent potassium phosphonate (phosphite). J. Gen. Microbiol. 136, 1285–1291.

Guimarães, R.L., Stotz, H.U., 2004. Oxalate production by *Sclerotinia sclerotiorum* deregulates guard cells during infection. Plant Physiol. 136, 3703–3711.

Guo, Y., Liu, L., Zhao, J., Bi, Y., 2007. Use of silicon oxide and sodium silicate for controlling *Trichothecium roseum* postharvest rot in Chinese cantaloupe (*Cucumis mel*o L.). Int. J. Food Sci. Technol. 42, 1012–1018.

Harman, G.E., Hayes, C.K., Lorito, M., Broadway, R.M., Di Pietro, A., Peterbauer, C., Tronsmo, A., 1993. Chitinolytic enzymes of *Trichoderma harzianum*: purification of chitobiosidase and endochitinase. Phytopathology 83, 313-318.

Heath, R.L., Packer, L., 1968. Photoperoxidation in isolated chloroplasts I. Kinetics and stoichiometry of fatty acid peroxidation. Arch. Biochem. Biophys. 125, 189–198.

Heffer Link, V., Johnson, K.B., 2007. White mold: the plant health instructor. http://www.apsnet.org/edcenter/disandpath/fungalasco/pdlessons/Pages/WhiteMold.aspx. Accessed on November 29, 2019.

Kabbage, M., Williams, B., Dickman, M.B., 2013. Cell death control: the interplay of apoptosis and autophagy in the pathogenicity of *Sclerotinia sclerotiorum*. PLoS Pathog. 9, e1003287.

Kar, M., Mishra, D., 1976. Catalase, peroxidase, and polyphenoloxidase activities during rice leaf senescence. Plant Physiol. 57, 315-319.

Kramer, D.M., Johnson, G., Kiirats, O., Edwards, G.E., 2004. New fluorescence parameters for the determination of Q_A redox state and excitation energy fluxes. Photosynth. Res. 79, 209-218.

Lehner, M.S., Paula Junior, T.J., Silva, R.A., Vieira, R.F., Carneiro, J.E.S., Schnabel, G., Mizubuti, E.S.G., 2015. Fungicide sensitivity of *Sclerotinia sclerotiorum*: A thorough assessment using discriminatory dose, EC_{50}, high-resolution melting analysis, and description of new point mutation associated with thiophanate-methyl resistance. Plant Dis. 99, 1537–1543.

Lever, M., 1972. A new reaction for colorimetric determination of carbohydrates. Anal. Biochem. 47, 273-279.

Liu, P., Li, B., Lin, M., Chen, G., Ding, X., Weng, Q., Chen, Q., 2016. Phosphite-induced reactive oxygen species production and ethylene and ABA biosynthesis, mediate the control of *Phytophthora capsici* in pepper (*Capsicum annuum*). Funct. Plant Biol. 43, 563-574.

Liu, S., Zhang, Y., Jiang, J., Che, Z., Tian, Y., Chen, G., 2018. Carbendazim resistance and dimethachlone sensitivity of field isolates of *Sclerotinia sclerotiorum* from oilseed rape in Henan Province, China. J. Phytopathol. 166, 701–708.

Lobato, M.C., Olivieri, F.P., Daleo, G.R., Andreu, A.B., 2010. Antimicrobial activity of phosphites against different potato pathogens. J. Plant Dis. Protect. 117, 102–109.

Lobo Junior, M., Lopes, C.A., Silva, W.L.C., 2000. Sclerotinia rot losses in processing tomatoes grown under centre pivot irrigation in central Brazil. Plant Pathol. 49, 51–56.

Malenčić, D., Kiprovski, B., Popović, M., Prvulović, D., Miladinović, J., Djordjević, V., 2010. Changes in antioxidant systems in soybean as affected by *Sclerotinia sclerotiorum* (Lib.) de Bary. Plant Physiol. Biochem. 48, 903–908.

Maxwell, K., Johnson, G.N., 2000. Chlorophyll fluorescence - a practical guide. J. Exp. Bot. 51, 659–668.

Meena, M., Zehra, A., Dubey, M.K., Aamir, M., Gupta, V.K., Upadhyay, R.S., 2016. Comparative evaluation of biochemical changes in tomato (*Lycopersicon esculentum* Mill.) infected by *Alternaria alternata* and its toxic metabolites (TeA, AOH, and AME). Front. Plant Sci. 7, 1408.

Mesquita, G.L., Tanaka, F.A.O., Zambrosi, F.C.B., Chapola, R., Cursi, D., Habermann, G., Massola Junior, N.S., Ferreira, V.P., Gaziola, S.A., Azevedo, R.A., 2019. Foliar application of manganese increases sugarcane resistance to orange rust. Plant Pathol. 68, 1296–1307.

Millaleo, R., Reyes-Díaz, M., Ivanov, A.G., Mora, M.L., Alberdi, M., 2010. Manganese as essential and toxic element for plants: transport, accumulation and resistance mechanisms. J. Soil Sci. Plant Nutr. 10, 476–494.

Monteiro, A.C.A., Resende, M.L.V., Valente, T.C.T., Ribeiro Junior, P.M., Pereira, V.F., Costa, J.R., Silva, J.A.G., 2016. Manganese phosphite in coffee defence against *Hemileia*

vastatrix, the coffee rust fungus: biochemical and molecular analyses. J. Phytopathol. 164, 1043–1053.

Mulugeta, T., Abreha, K., Tekie, H., Mulatu, B., Yesuf, M., Andreasson, E., Liljeroth, E., Alexandersson, E., 2019. Phosphite protects against potato and tomato late blight in tropical climates and has varying toxicity depending on the *Phytophthora infestans* isolate. Crop Prot. 121, 139–146.

Nakano, Y., Asada, K., 1981. Hydrogen peroxide is scavenged by ascorbate-specific peroxidase in spinach chloroplasts. Plant Cell Physiol. 22, 867-880.

Nascimento, K.J.T., Araujo, L., Resende, R.S., Schurt, D.A., Silva, W.L., Rodrigues, F.A., 2016. Silicon, acibenzolar-S-methyl and potassium phosphite in the control of brown spot in rice. Bragantia 75, 212–221.

Niere, J.O., DeAngelis, G., Grant, B.R., 1994. The effect of phosphonate on the acid-soluble phosphorus components in the genus *Phytophthora*. Microbiology 140, 1661–1670.

Novaes, M.I.C., Debona, D., Fagundes-Nacarath, I.R.F., Brás, V.V., Rodrigues, F.A., 2019. Physiological and biochemical responses of soybean to white mold affected by manganese phosphite and fluazinam. Acta Physiol. Plant. 41, 186.

Oxborough, K., Baker, N.R., 1997. Resolving chlorophyll *a* fluorescence images of photosynthetic efficiency into photochemical and non-photochemical components - calculation of *qP* and *Fv*'/*Fm*' without measuring *Fo*'. Photosynth. Res. 54, 135–142.

Percival, G.C., Banks, J.M., 2015. Phosphite-induced suppression of *Pseudomonas* bleeding canker (*Pseudomonas syringae* pv. *aesculi*) of horse chestnut (*Aesculus hippocastanum* L.). Urban For. Urban Green. 37, 7–20.

Rios, J.A., Aucique-Pérez, C.E., Debona, D., Cruz Neto, L.B.M., Rios, V.S., Rodrigues, F.A., 2017. Changes in leaf gas exchange, chlorophyll *a* fluorescence and antioxidant metabolism within wheat leaves infected by *Bipolaris sorokiniana*. Ann. Appl. Biol. 170, 189–203.

Rios, V.S., Rios, J.A., Aucique-Pérez, C.E., Silveira, P.R., Barros, A.V., Rodrigues, F.A., 2018. Leaf gas exchange and chlorophyll *a* fluorescence in soybean leaves infected by *Phakopsora pachyrhizi*. J. Phytopathol. 166, 75–85.

Sánchez-Vallet, A., Mesters, J.R., Thomma, B.P.H.J., 2015. The battle for chitin recognition in plant-microbe interactions. FEMS Microbiol. Rev. 39, 171–183.

Shaner, G., Finney, R.E., 1977. The effect of nitrogen fertilization on the expression of slow-mildewing resistance in knox wheat. Phytopathology 67, 1051-1055.

Sharma, P., Jha, A.B., Dubey, R.S., Pessarakli, M., 2012. Reactive oxygen species, oxidative damage, and antioxidative defense mechanism in plants under stressful conditions. J. Bot. 2012, 1–26.

Silveira, P.R., Nascimento, K.J.T., Andrade, C.C.L., Bispo, W.M.S., Oliveira, J.R., Rodrigues, F.A., 2015. Physiological changes in tomato leaves arising from *Xanthomonas gardneri* infection. Physiol. Mol. Plant Pathol. 92, 130–138.

Tariq, V.N., Jeffries, P., 1985. Changes occurring in chloroplasts of *Phaseolus* following infection by *Sclerotinia*: a cytochemical study. J. Cell Sci. 75, 195–205.

Tatagiba, S.D., DaMatta, F.M., Rodrigues, F.A., 2015. Leaf gas exchange and chlorophyll *a* fluorescence imaging of rice leaves infected with *Monographella albescens*. Phytopathology 105, 180–188.

Vale, F.X.R., Fernandes Filho, E.I., Liberato, J.R., 2003. QUANT: a software plant disease severity assessment. In: Close R, Braithwaite M, Havery I, eds. Proceedings of 8th International Congress of Plant Pathology, New Zealand. p.105.

Vallad, G.E., Goodman, R.M., 2004. Systemic acquired resistance and induced systemic resistance in conventional agriculture. Crop Sci. 44, 1920–1934.

Velikova, V., Yordanov, I., Edreva, A., 2000. Oxidative stress and some antioxidant systems in acid rain-treated bean plants: protective role of exogenous polyamines. Plant Sci. 151, 59–66.

Veluchamy, S., Williams, B., Kim, K., Dickman, M.B., 2012. The CuZn superoxide dismutase from *Sclerotinia sclerotiorum* is involved with oxidative stress tolerance, virulence, and oxalate production. Physiol. Mol. Plant Pathol. 78, 14–23.

Walters, D.R., Ratsep, J., Havis, N.D., 2013. Controlling crop diseases using induced resistance: challenges for the future. J. Exp. Bot. 64, 1263–1280.

Wellburn, A.R., 1994. The spectral determination of chlorophylls *a* and *b,* as well as total carotenoids, using various solvents with spectrophotometers of different resolution. J. Plant Physiol. 144, 307–313.

Willbur, J., McCaghey, M., Kabbage, M., Smith, D.L., 2019. An overview of the *Sclerotinia sclerotiorum* pathosystem in soybean: impact, fungal biology, and current management strategies. Trop. Plant Pathol. 44, 3–11.

Williams, B., Kabbage, M., Kim, H.J., Britt, R., Dickman, M.B., 2011. Tipping the balance: *Sclerotinia sclerotiorum* secreted oxalic acid suppresses host defenses by manipulating the host redox environment. PLoS Pathog. 7, e1002107.

Yang, C., Zhang, Z., Gao, H., Liu, M., Fan, X., 2014. Mechanisms by which the infection of *Sclerotinia sclerotiorum* (Lib.) de Bary affects the photosynthetic performance in tobacco leaves. BMC Plant Biol. 14, 240.

Yao, Y.A., Wang, J., Ma, X., Lutts, S., Sun, C., Ma, J., Yang, Y., Achal, V., Xu, G., 2012. Proteomic analysis of Mn-induced resistance to powdery mildew in grapevine. J. Exp. Bot. 63, 5155-5170.

You, J., Chan, Z., 2015. ROS regulation during abiotic stress responses in crop plants. Frontiers in Plant Sci. 6, 1092.

TABLE AND FIGURES

Table 1. Analysis of variance of the effects of foliar treatments (FT), plant inoculation (PI), evaluation time (ET), and their interactions for white mold severity (WMS), area under disease progress curve (AUDPC), foliar manganese (Mn) concentration, leaf gas exchange parameters (net CO_2 assimilation rate (A), stomatal conductance to water vapor (g_s), internal to ambient CO_2 concentration ratio (C_i/C_a), and transpiration rate (E)), chlorophyll (Chl) *a* fluorescence parameters (maximum fluorescence (F_m), maximum PSII quantum efficiency (F_v/F_m), photochemical yield (Y(II)), yield for dissipation by down-regulation (Y(NPQ)) and yield for other non-photochemical (non-regulated) losses (Y(NO)), and electron transport rate (ETR)), concentrations of chlorophyll *a+b* (Chl *a+b*) and carotenoids (CAR), activities of antioxidant (superoxide dismutase (SOD), catalase (CAT), peroxidase (POX), ascorbate peroxidase (APX), glutathione-reductase (GR)) and activities of defense-related enzymes ((chitinase (CHI), β-1,3-glucanase (GLU), phenylalanine ammonia-lyase (PAL), polyphenoloxidase (PPO) and lipoxygenase (LOX)), as well as for the concentrations of superoxide (O_2^-), hydrogen peroxide (H_2O_2), and malondialdehyde (MDA).

Variables/Parameters	FT	PI	ET	FT × PI	FT × ET	PI × ET	FT × PI × ET
WMS	<0.001	-	<0.001	-	<0.001	-	-
AUDPC	<0.001	-	-	-	-	-	-
Mn	0.003	0.665	-	0.430	-	-	-
A	0.536	<0.001	<0.001	0.145	0.388	<0.001	0.202
g_s	0.054	0.007	0.001	0.300	0.099	0.005	0.997
C_i/C_a	0.437	<0.001	0.035	0.307	0.490	0.916	0.689
E	0.028	0.591	<0.001	0.002	0.005	0.005	0.367
F_m	<0.001	<0.001	<0.001	<0.001	0.399	<0.001	0.016
F_v/F_m	<0.001	<0.001	<0.001	<0.001	<0.001	<0.001	<0.001
Y(II)	<0.001	<0.001	<0.001	<0.001	<0.001	<0.001	0.001
Y(NPQ)	0.028	<0.001	<0.001	0.002	0.507	<0.001	0.009
Y(NO)	<0.001	<0.001	<0.001	<0.001	<0.001	<0.001	0.001
ETR	<0.001	<0.001	<0.001	<0.001	<0.001	<0.001	<0.001
Chl $a + b$	<0.001	0.008	<0.001	0.018	0.003	<0.001	0.017
CAR	<0.001	0.354	<0.001	0.003	0.001	0.004	0.007
SOD	0.008	0.017	0.001	0.009	0.454	0.001	0.070
APX	0.243	<0.001	0.017	0.237	0.185	0.059	0.007
CAT	<0.001	0.002	<0.001	0.002	0.134	0.043	0.123
POX	<0.001	<0.001	<0.001	0.004	0.056	<0.001	0.109
GR	0.001	0.077	<0.001	0.015	0.005	0.069	0.181
CHI	<0.001	0.076	0.002	0.074	0.495	0.002	0.753
GLU	<0.001	<0.001	<0.001	0.001	0.056	0.002	0.408
PAL	0.196	0.051	0.001	0.396	0.903	<0.001	0.037
PPO	0.051	0.003	0.003	0.065	0.353	0.216	0.118
LOX	0.017	0.001	<0.001	0.001	0.006	0.016	0.052
O_2^-	0.024	<0.001	<0.001	0.019	0.063	0.022	0.362
H_2O_2	0.435	0.306	0.018	0.044	0.831	0.069	0.136
MDA	<0.001	<0.001	<0.001	<0.001	0.001	<0.001	0.014

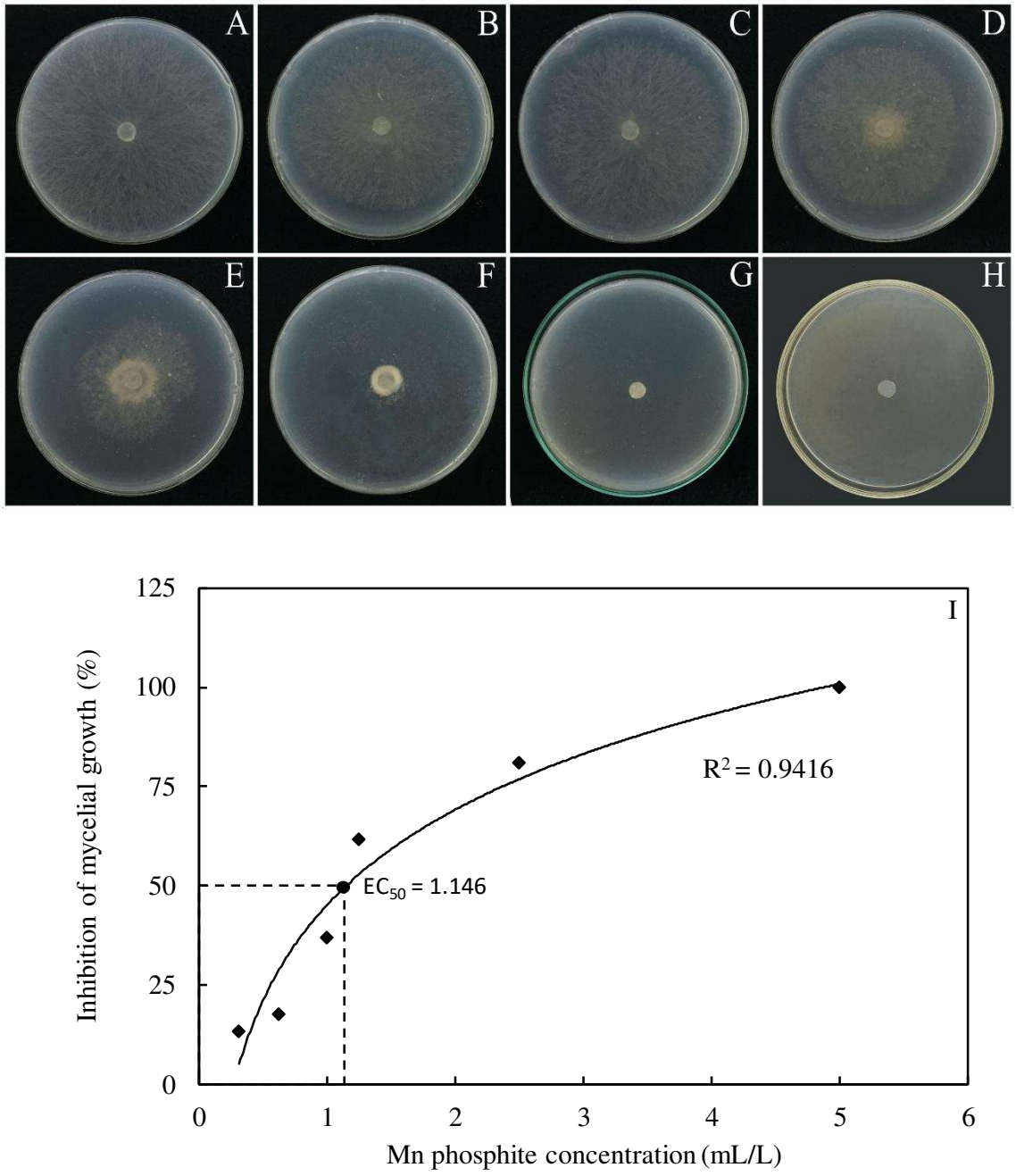

Figure 1. Mycelial growth of *Scletorotinia sclerotiorum* in Petri dishes containing potato-dextrose-agar amended with 0 (A), 0.3125 (B), 0.625 (C), 1 (D), 1.25 (E), 2.5 (F), and 5 (G) mL L^{-1} of manganese phosphite and 1.25 mL L^{-1} (H) of the fungicide Fluazinam. Effective concentration (EC_{50}) of manganese (Mn) phosphites that inhibited 50% of mycelial growth of *Sclerotinia sclerotiorum* (I).

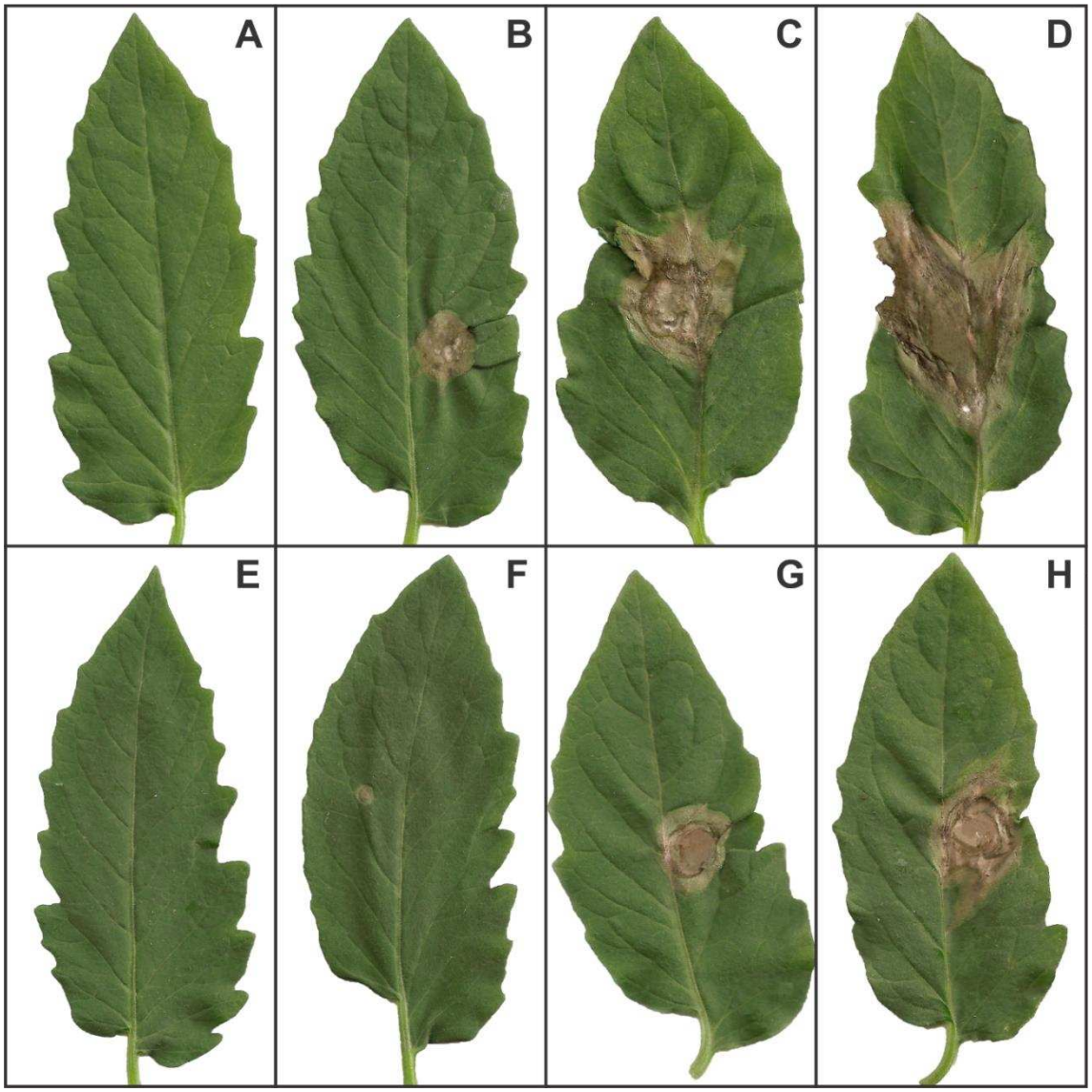

Figure 2. White mold symptoms at 24 (A and E), 36 (B and F), 60 (C and G), and 84 (D and H) hours after inoculation of tomato plants with *Sclerotinia sclerotiorum* and sprayed with water (control) (A-D) or with manganese (Mn) phosphite (E-H)

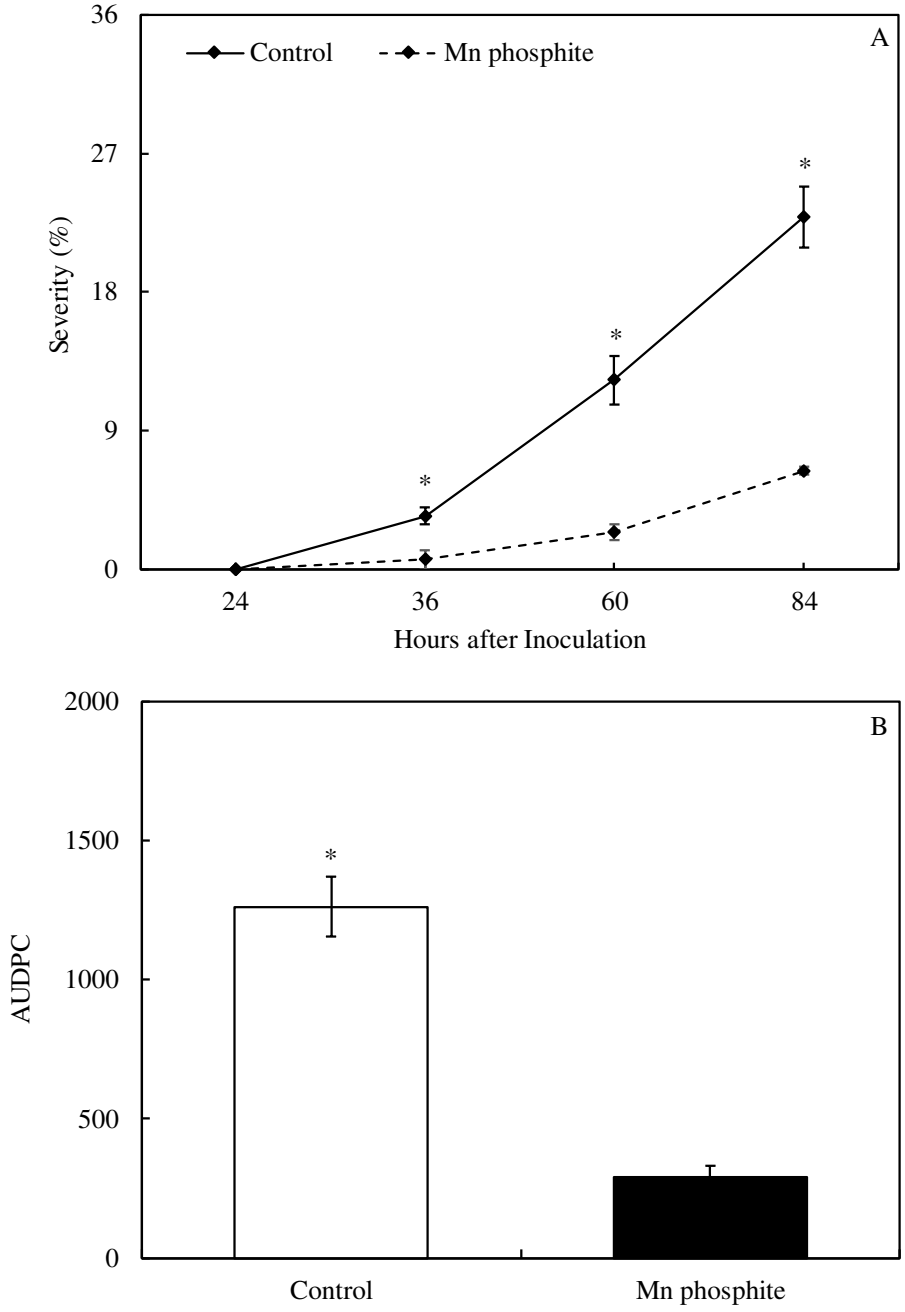

Figure 3. White mold severity (A) and area under disease progress curve (AUDPC) (B) for tomato plants sprayed with water (control) or with manganese (Mn) phosphite. Means from each treatment followed by an asterisk (*) at each evaluation time (A) and between treatments (B) are significantly different ($P \leq 0.05$) by F test. Bars represent the standard error of the means. $n = 4$.

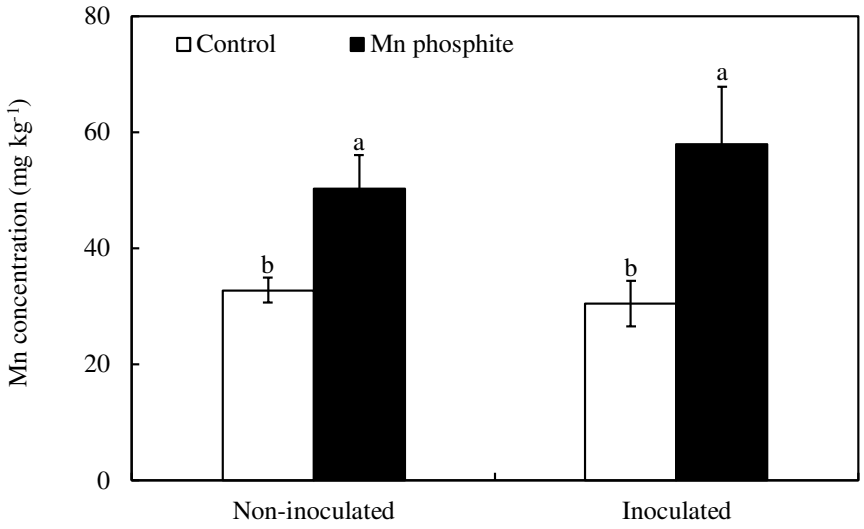

Figure 4. Foliar manganese (Mn) concentration for tomato plants non-inoculated (NI) or inoculated (I) with *Sclerotinia sclerotiorum* and sprayed with water (control) or with manganese (Mn) phosphite. Means from treatments for either NI or I plants followed by different letters are significantly different ($P \leq 0.05$) by F test. Bars represent the standard error of the means. $n = 4$.

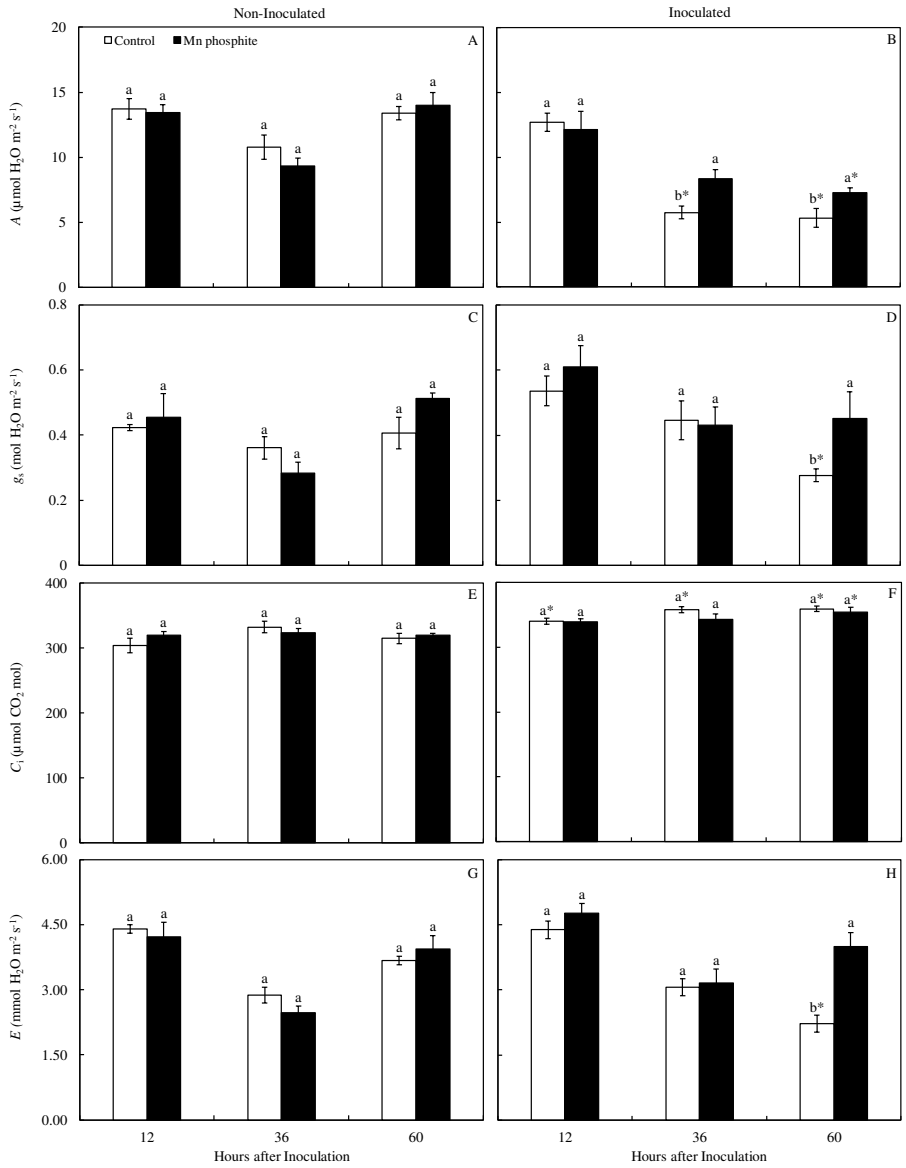

Figure 5. Leaf gas exchange parameters: net carbon assimilation rate (*A*) (A and B), stomatal conductance to water vapor (g_s) (C and D), internal CO_2 concentration (C_i) (E and F), and transpiration rate (*E*) (G and H) determined on the leaflets of tomato plants non-inoculated (A, C, E, and G) or inoculated (B, D, F, and H) with *Sclerotinia sclerotiorum* and sprayed with water (control) or with manganese (Mn) phosphite. For each evaluation time, means from each treatment followed by different letters and from non-inoculated and inoculated plants for each treatment followed by an asterisk (*) are significantly different ($P \leq 0.05$) by *F* test. Bars represent the standard error of the means. $n = 4$.

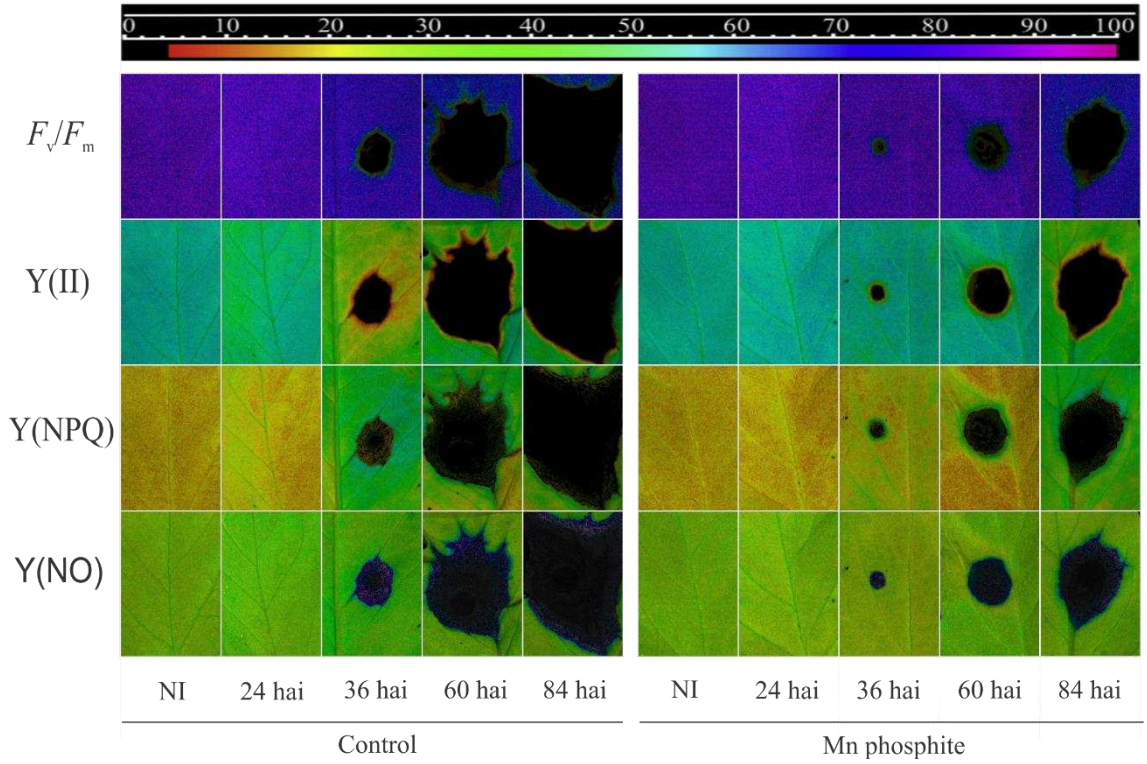

Figure 6. Images of chlorophyll *a* fluorescence parameters: maximum PSII quantum efficiency (F_v/F_m), photochemical yield (Y(II)), yield for dissipation by down-regulation (Y(NPQ)), and yield for non-regulated dissipation (Y(NO)) determined on the leaflets of tomato plants sprayed with water (control) or with manganese (Mn) phosphite and non-inoculated (NI) and at 24, 36, 60, and 84 hours after inoculation (hai) with *Sclerotinia sclerotiorum*.

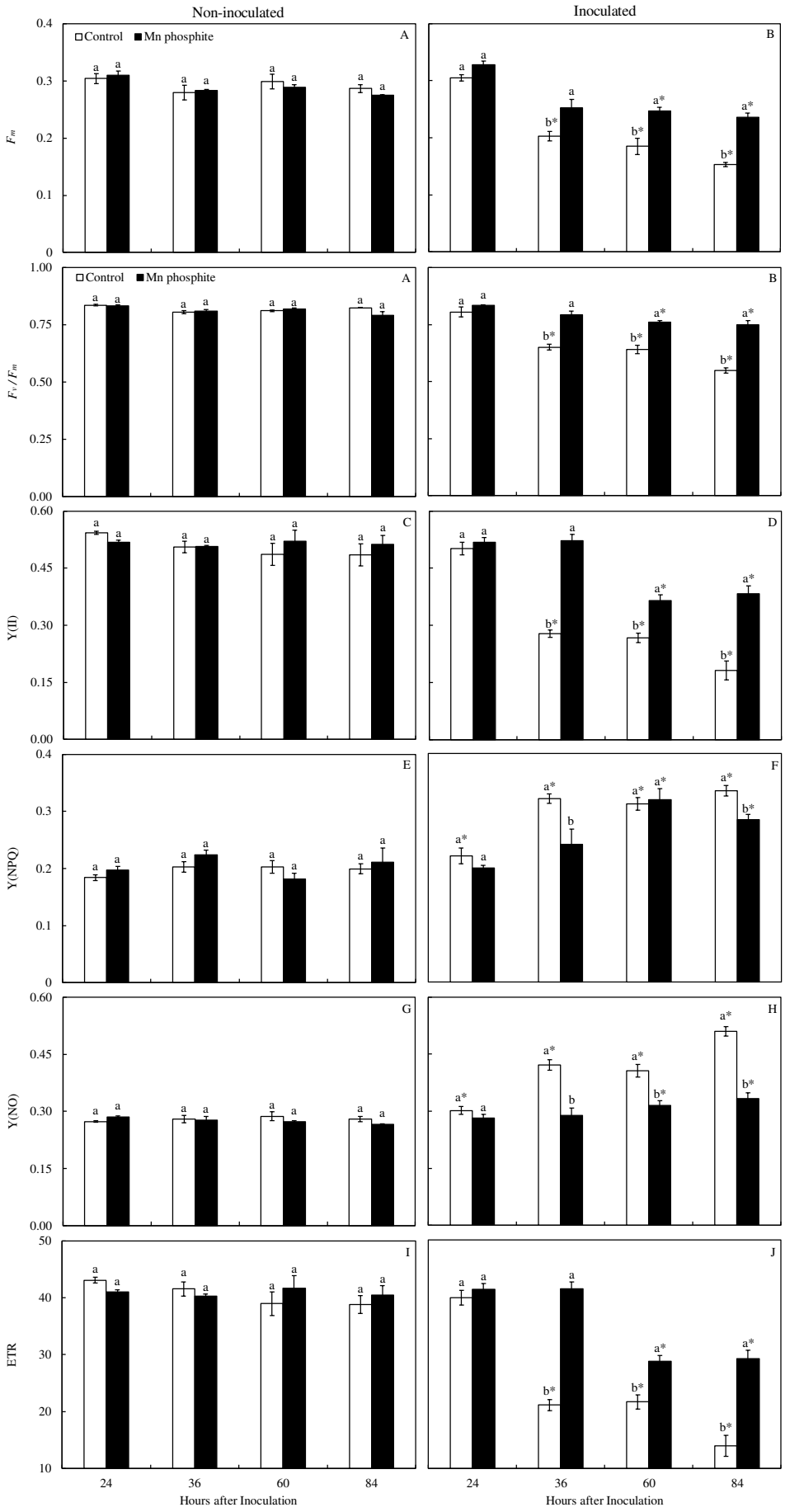
Non-inoculated
Inoculated
Control
Mn phosphite
A
B
C
D
E
F
G
H
I
J
F_m
F_v/F_m
Y(II)
Y(NPQ)
Y(NO)
ETR
Hours after Inoculation
Hours after Inoculation

Figure 7. Chlorophyll *a* parameters: maximum PSII quantum efficiency (F_v/F_m) (A and B), photochemical yield (Y(II)) (C and D), yield for dissipation by down-regulation (Y(NPQ)) (E and F), yield for other non-photochemical (non-regulated) losses (Y(NO)) (G and H), and electron transport rate (ETR) (I and J) determined on the leaflets of tomato plants non-inoculated (A, C, E, G, and I) or inoculated (B, D, F, H, and J) with *Sclerotinia sclerotiorum* and sprayed with water (control) or with manganese (Mn) phosphite. For each evaluation time, means from each treatment followed by different letters and from non-inoculated and inoculated plants for each treatment followed by an asterisk (*) are significantly different ($P \leq 0.05$) by *F* test. Bars represent the standard error of the means. $n = 4$.

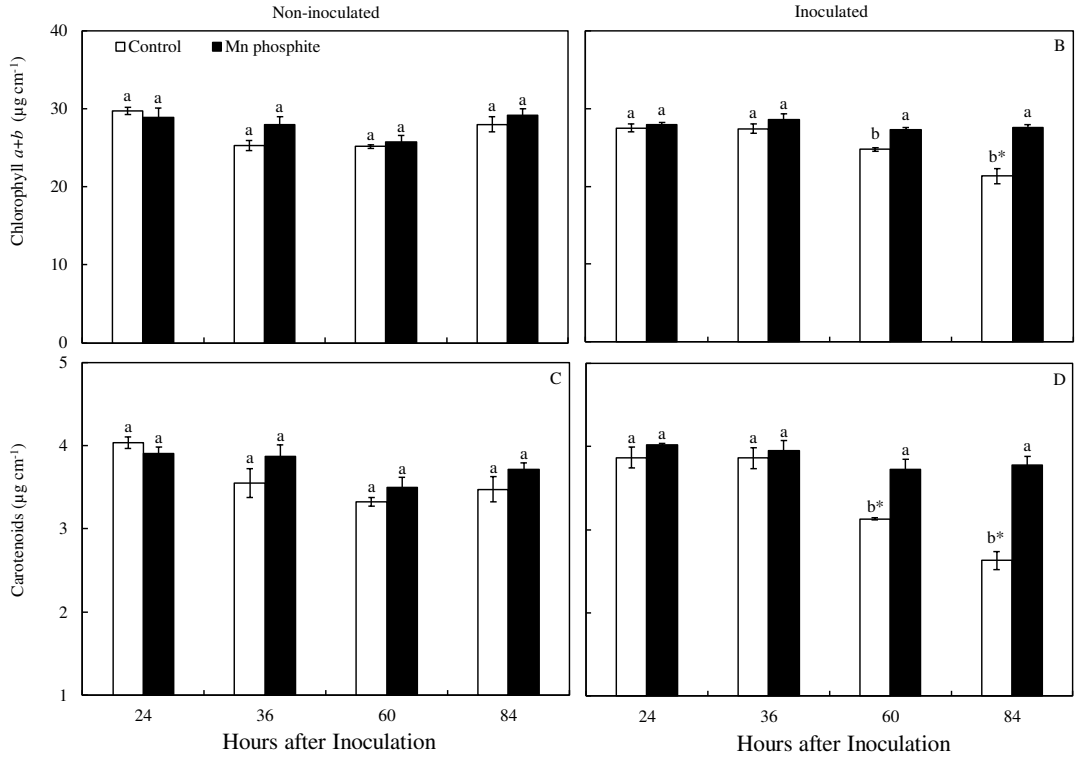

Figure 8. Concentrations of chlorophylls *a* + *b* (Chl *a*+*b*) (A and B) and carotenoids (C and D) determined on the leaflets of tomato plants non-inoculated (A and C) or inoculated (B and D) with *Sclerotinia sclerotiorum* and sprayed with water (control) or with manganese (Mn) phosphite. For each evaluation time, means from each treatment followed by different letters and from non-inoculated and inoculated plants for each treatment followed by an asterisk (*) are significantly different ($P \leq 0.05$) by *F* test. Bars represent the standard error of the means. $n = 4$.

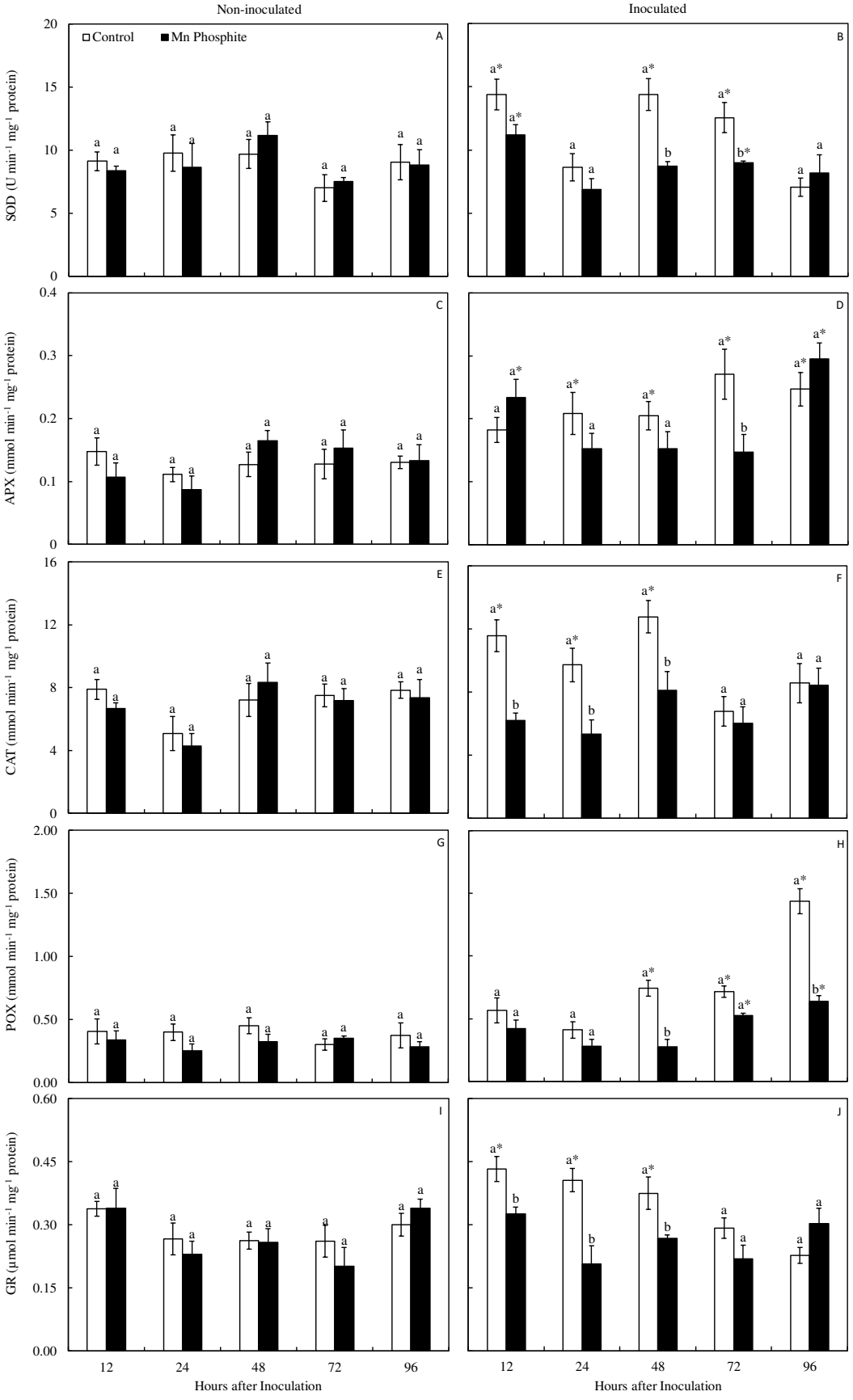
Non-inoculated
Inoculated
Control
Mn Phosphite
A
B
C
D
E
F
G
H
I
J
SOD (U min-1 mg-1 protein)
APX (mmol min-1 mg-1 protein)
CAT (mmol mim-1 mg-1 protein)
POX (mmol min-1 mg-1 protein)
GR (μmol min-1 mg-1 protein)
Hours after Inoculation
Hours after Inoculation

Figure 9. Activities of superoxide dismutase (SOD) (A and B), ascorbate peroxidase (APX) (C and D), catalase (CAT) (E and F), peroxidase (POX) (G and H), and glutathione reductase (GR) (I and J) determined on the leaflets of tomato plants non-inoculated (A, C, E, G, and I) or inoculated (B, D, F, H, and J) with *Sclerotinia sclerotiorum* and sprayed with water(control) or with manganese (Mn) phosphite. For each evaluation time, means from each treatment followed by different letters and for non-inoculated and inoculated plants for each treatment followed by an asterisk (*) are significantly different ($P \leq 0.05$) based on *F* test. Bars represent the standard error of the means. $n = 4$.

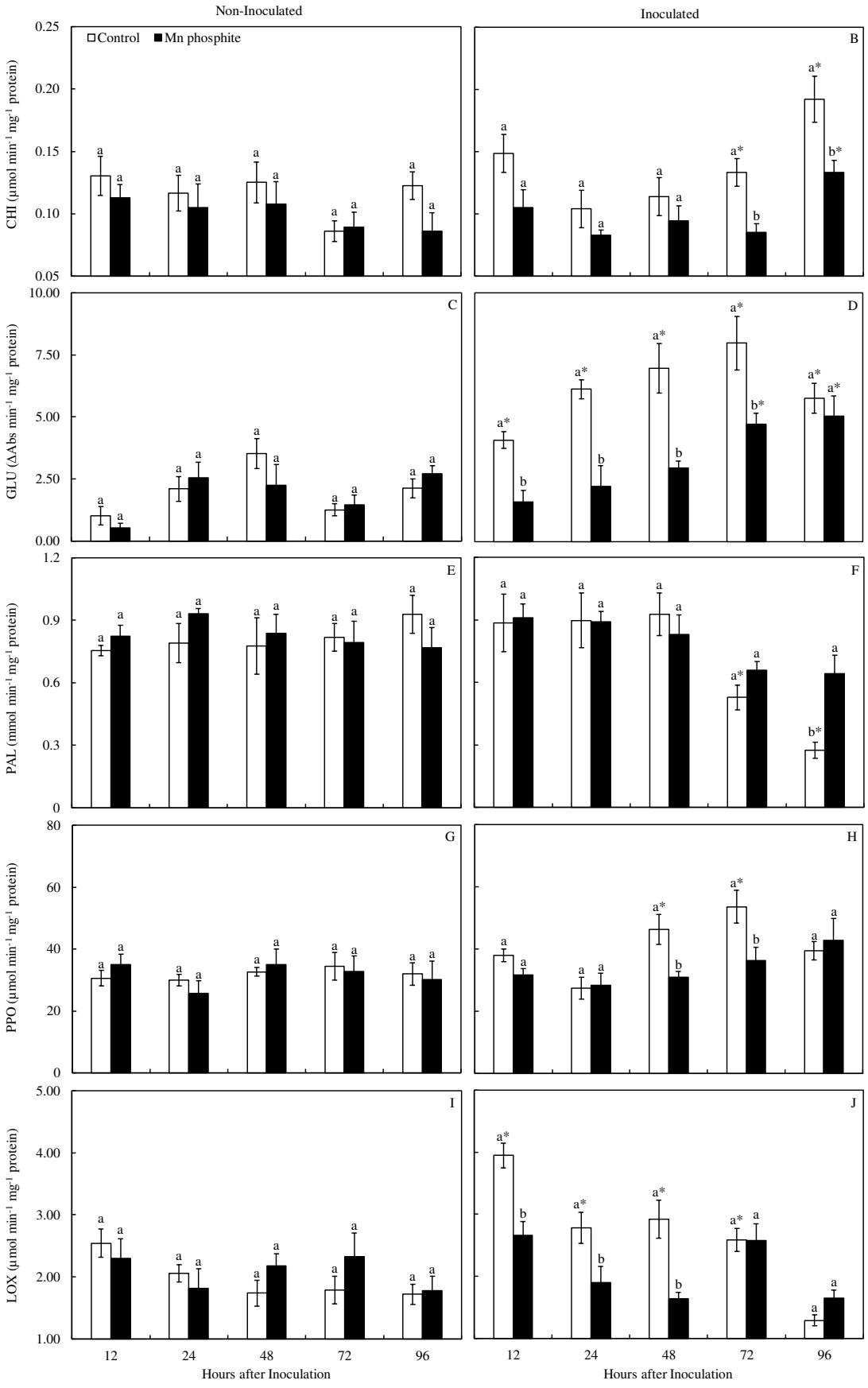
Non-Inoculated
Inoculated
Control
Mn phosphite
CHI (µmol min-1 mg-1 protein)
GLU (ΔAbs min-1 mg-1 protein)
PAL (mmol min-1 mg-1 protein)
PPO (µmol min-1 mg-1 protein)
LOX (µmol min-1 mg-1 protein)
Hours after Inoculation
Hours after Inoculation

Figure 10. Activities of chitinase (CHI) (A and B), β-1,3-glucanase (GLU) (C and D), phenylalanine ammonia-lyase (PAL) (E and F), polyphenoloxidase (PPO) (G and H), and lipoxygenase (LOX) (I and J) determined on the leaflets of tomato plants non-inoculated (A, C, E, and G) or inoculated (B, D, F, and H) with *Sclerotinia sclerotiorum* and sprayed with water (control) or with manganese (Mn) phosphite. For each evaluation time, means from each treatment followed by different letters and from non-inoculated and inoculated plants for each treatment followed by an asterisk (*) are significantly different ($P \leq 0.05$) by F test. Bars represent the standard error of the means. $n = 4$.

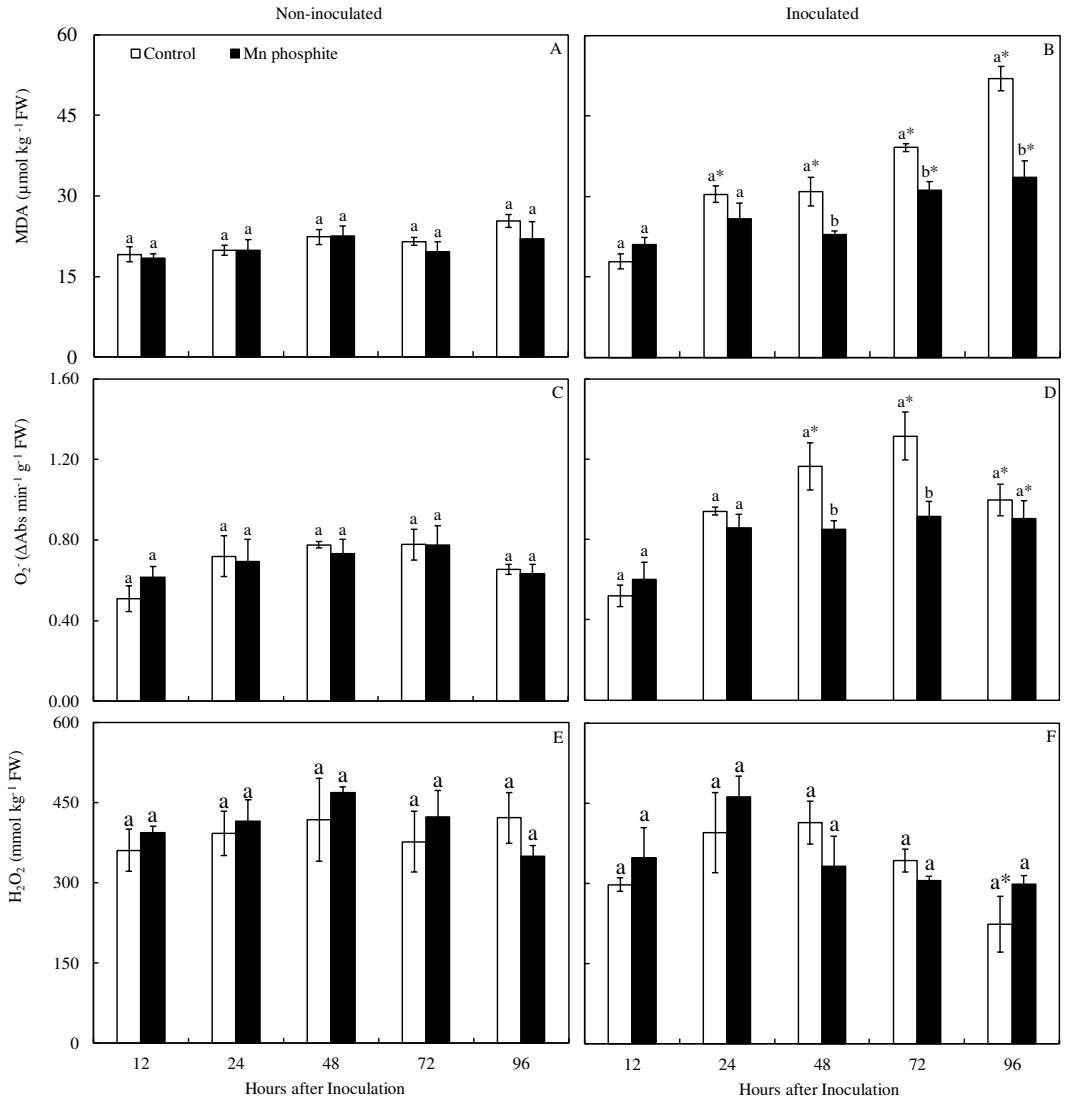

Figure 11. Concentrations of malondialdehyde (MDA) (A and B), superoxide (O_2^-) (C and D), and hydrogen peroxide (H_2O_2) (E and F) determined on the leaflets of tomato plants non-inoculated (A, C, and E) or inoculated (B, D, and F) with *Sclerotinia sclerotiorum* and sprayed with water (control) or with manganese (Mn) phosphite. For each evaluation time, means from each treatment followed by different letters and from non-inoculated and inoculated plants for each treatment followed by an asterisk (*) are significantly different ($P \leq 0.05$) by *F* test. Bars represent the standard error of the means. FW = fresh weight. $n = 4$.